NUREG/CR-2188

Simulation of Sodium Pumps for Nuclear Power Plants

Prepared by H. O. Boadu

Department of Nuclear and Energy Engineering
The University of Arizona

Prepared for
U.S. Nuclear Regulatory Commission

Available from

GPO Sales Program
Division of Technical Information and Document Control
U. S. Nuclear Regulatory Commission
Washington, D. C. 20555

Printed copy price: $4.00

and

National Technical Information Service
Springfield, Virginia 22161

NUREG/CR-2188
R7

Simulation of Sodium Pumps for Nuclear Power Plants

Manuscript Completed: May 1981
Date Published: August 1981

Prepared by
H. O. Boadu

Department of Nuclear and Energy Engineering
The University of Arizona
Tucson, AZ 85721

Prepared for
Division of Accident Evaluation
Office of Nuclear Regulatory Research
U.S. Nuclear Regulatory Commission
Washington, D.C. 20555
NRC FIN A4065

ABSTRACT

A single-phase pump model for analysis of transients in sodium cooled fast breeder nuclear power plants has been presented, where homologous characteristic curves are used to predict the behavior of the pump during operating transients. The pump model has been incorporated into BRENDA and FFTF; two system cases to simulate Clinch River Breeder Reactor Plant (CRBRP) and the Fast Flux Test Facility (FFTF) respectively. Two simulation test results for BRENDA which is one loop representation of a three loop plant have been presented. They are:

i) Primary pump coastdown to natural circulation coupled with scram failure.

ii) 10 percent deviation of primary speed with plant controllers incorporated.

In the case of FFTF, which is a two loop representation of three loop physical plant, the results of a 10 percent step decrease in one of the pumps will be presented.

TABLE OF CONTENTS

LIST OF ILLUSTRATIONS

LIST OF TABLES

LIST OF VARIABLES

Symbol	Parameter	Units
EN	normalized reactor power in BRENDA	
g	acceleration due to gravity	ft/s^2
h	normalized pump head (H/H_R)	
H	pump head	ft
I	moment of inertia	$lb_f\text{-}ft\text{-}s^2/rad^2$
N	pump speed	RPM
PUMP 1	pump head in loop one (FFTF)	ft
PUMP 2	pump head in loop two (FFTF)	ft
Q	pump volumetric discharge	ft^3/s
WI	intermediate sodium flow rate (BRENDA)	lb_m/hr
WL11	vessel-to-pump flow rate (FFTF loop one)	lb_m/hr
WL12	pump-to-IHX flow rate (FFTF loop one)	lb_m/hr
WL13	IHX-to-vessel flow rate (FFTF loop one)	lb_m/hr
WL21	vessel-to-pump flow rate (FFTF loop two)	lb_m/hr
WL22	pump-to-IHX flow rate (FFTF loop two)	lb_m/hr
WL23	IHX-to-vessel flow rate (FFTF loop two)	lb_m/hr
WP	primary sodium flow rate (BRENDA)	lb_m/hr
TIA	temperature of sodium entering the superheater	°F
T_{p5}	temperature of sodium entering the IHX on the primary loop side	°F
T_{s9}	temperature of steam entering the turbine	°F

LIST OF VARIABLES--Continued

Symbol	Parameter	Units
α	normalized pump speed (N/N_R)	
β	normalized hydraulic torque (τ_{hyd}/τ_R)	
ν	normalized pump discharge (Q/Q_R)	
ρ	coolant density	lb_m/ft^3
τ	torque	lb_f-ft/rad

ACKNOWLEDGMENTS

The author acknowledge the support of the Division of Reactor Safety Research, United States Nuclear Regulatory Commission for financial support under Contract NRC-04-250. He is indebted to Dr. David L. Hetrick, Principal Investigator, for the many hours of discussion involved in completion of this thesis. Finally, the author is deeply grateful to Dr. P. V. Girijashankar for his excellent guidance in all phases of this thesis.

CHAPTER 1

INTRODUCTION

1.1 Background and Objective

The primary concern in the safety analysis of a liquid metal cooled fast breeder reactor (LMFBR) system is whether adequate cooling capability is provided to maintain the fuel element temperatures below specified values during off-normal and accident events that may be postulated to occur in the heat transport system, e.g., loss of all pumping power. The behavior of the centrifugal pumps which circulate the reactor coolant becomes extremely important during such transients, and the ability to predict pump performance is necessary to understand and predict the interrelated hydraulic phenomena controlling loop and core flow rates. As an example, in the loss-of-flow accident caused by a power failure to all the coolant pumps, the flow coasts down and the system loses driving capability of flow through the core. The central question then becomes whether the power can be reduced rapidly enough such that the power-flow mismatch during the transient does not lead to unacceptable coolant temperatures. To answer the concern regarding core coolability, it is necessary to know how the pumps perform in the primary system. During the normal operation of the pump, both flow and speed are in the positive direction. However, during severe transients, the flow through the pump may completely reverse direction, as can the rotation, causing the pump to go through several regimes of operation. Therefore, analysis is required that

takes into account the changes occurring in the characteristics as the speed and flow change.

The objective of this work is to obtain a model for the pump which includes all the possible operating regimes of a pump and then to include it in the fast reactor system models for the Clinch River Breeder Reactor Plant (CRBRP) and the Fast Flux Test Facility (FFTF) to obtain their complete response.

A complete dynamic simulation of a liquid metal cooled fast breeder reactor (LMFBR) plant is an important part of the overall plant safety evaluation. A simplified diagram which has been used to model and study the dynamic behavior of the Clinch River Breeder Reactor Plant (CRBRP) (Shinaishin, 1976) using the simulation code named BRENDA (Hetrick and Sowers, 1978) is shown in Figure 1.1. The primary loop consists of the reactor, the primary coolant pump, and the intermediate heat exchanger (IHX). Liquid sodium is pumped from the reactor outlet plenum through the IHX, where it transfers heat to sodium flowing in the intermediate loop. The primary sodium returns to the reactor through the inlet plenum at the bottom of the reactor vessel. Sodium is the medium by which heat transfer takes place in the first two loops, and water is used in the third loop. Steam generated in the tertiary loop is then used to drive a conventional turbine. Although the simplified sketch shows one IHX, an evaporator and one superheater as forming one representative loop, the plant contains three such loops. Each heat transport loop has one variable speed primary pump located in the primary hot leg, one variable speed intermediate pump in the intermediate cold leg, and a constant speed recirculation pump in the down-comer from

Temperatures (°F)

$\bar{T}_{AF}$	(2202.7)	Average fuel
T_{IA}	(936.0)	Sodium entering superheater
T_{IC}	(856.0)	Sodium leaving superheater
T_{I7}	(856.0)	Sodium entering evaporator
T_{I9}	(651.0)	Sodium leaving evaporator
T_{I1}	(651.0)	Sodium entering IHX
T_{I3}	(936.0)	Sodium leaving IHX
T_{P4}	(994.73)	Sodium leaving the reactor
T_{P5}	(994.73)	Sodium entering IHX
T_{P7}	(730.0)	Sodium leaving IHX
T_{R1}	(730.0)	Sodium entering reactor
T_{SA}	(613.38)	Steam entering superheater
T_{SC}	(906.53)	Steam leaving superheater
T_{S9}	(901.7)	Steam entering turbine

Flow (lb_m/sec)

W_P	(11512.8)	Primary sodium
W_I	(10650.0)	Intermediate sodium
m_4	(1850.0)	Two phase entering drum
m_5	(925.0)	Feedwater entering drum
m_6	(1850.0)	Recirculation water leaving drum
m_7	(925.0)	Steam leaving drum
W_{S9}	(925.0)	Steam entering turbine

Miscellaneous

P	(1904.65)	Drum pressure psia
x_4	(.5)	Quality of steam at drum entrance
Y_{S5}	(3)	Water level in drum ft.

Fig. 1.1 Simplified Diagram of an LMFBR as Modelled by BRENDA

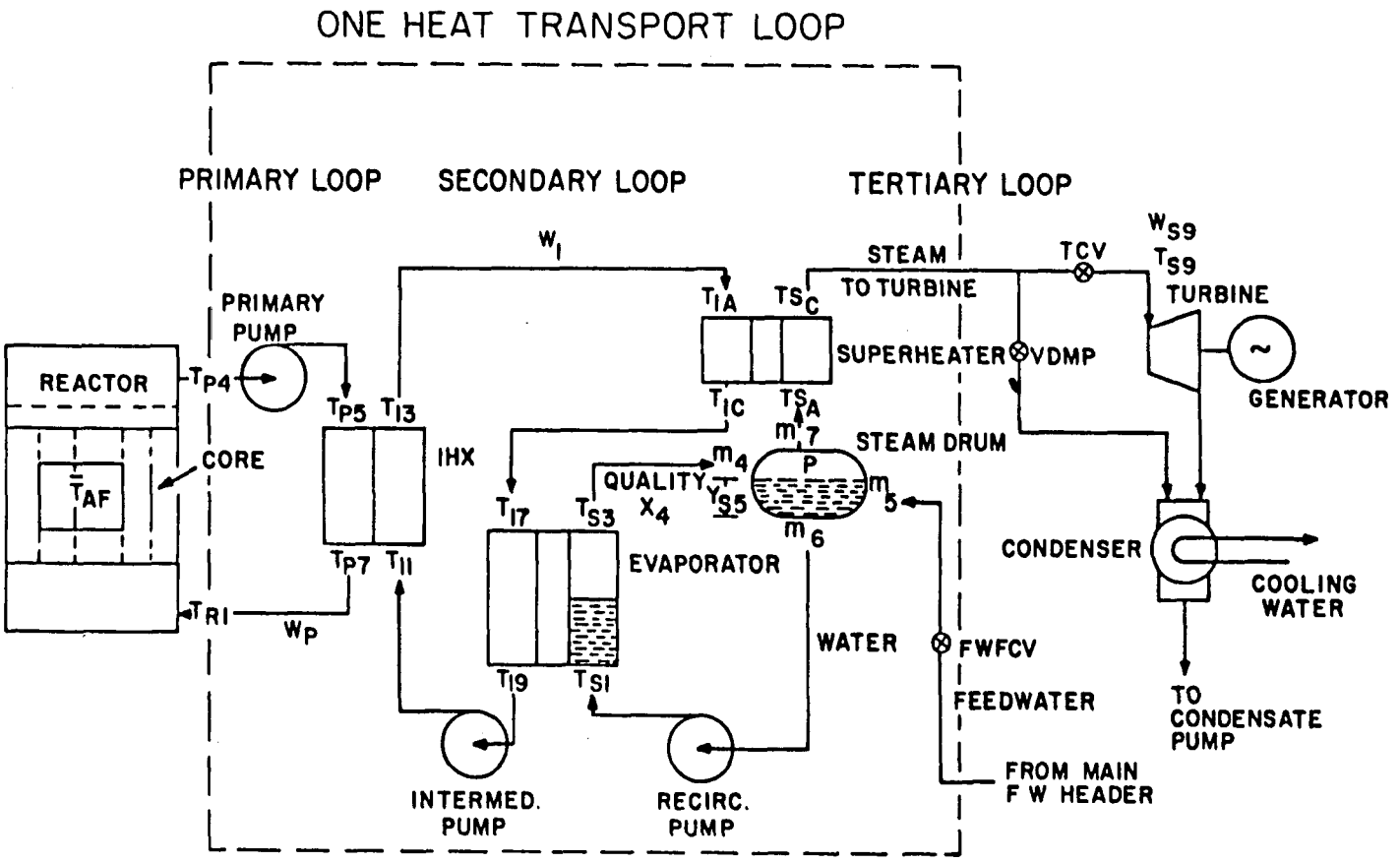

Fig. 1.1 -- Continued Simplified Diagram of an LMFBR as Modelled by BRENDA

the steam drum. In BRENDA a one-loop simulation with all three loops lumped together has been formed. BRENDA simulates the Clinch River Breeder Reactor Plant in enough detail to predict plant behavior for small transients by separately modelling the components and then combining them to form a complete plant simulation. The performance characteristics for sodium pumps have been represented by numerical tables for only the normal operating zone. This has not been good enough since the pump can reverse rotation and can also go through several other regimes of operation (Madni and Cazzoli, 1978). While the fundamental equations of the pump model are angular momentum balance and flow momentum balance for the primary loop to determine the flow in the loop and the pump speed, the new model allows reverse rotation and covers all regions of pump operation by representing the pump characteristics by homologous relations. The influence of frictional torque has also been incorporated. Results of simulations for pump coast down to natural circulation and a 10 percent set point change in the primary speed have been obtained.

The pump model has also been used in the Fast Flux Test Facility, a schematic simplified diagram of which is shown in Figure 1.2. Each loop has an intermediate heat exchanger (IHX) which is part of the primary coolant boundary and through which heat is transferred from the primary to the secondary coolant loop. The secondary coolant system then transports the heat to a dump-heat-exchanger (DHX) which rejects the thermal energy to the atmosphere. In the first version of this simulation the primary pumps have been modelled as constant speed pumps.

LEGEND

IHX Intermediate Heat Exchanger

DHX Dump Heat Exchanger

UP Upper Plenum

LP Lower Plenum

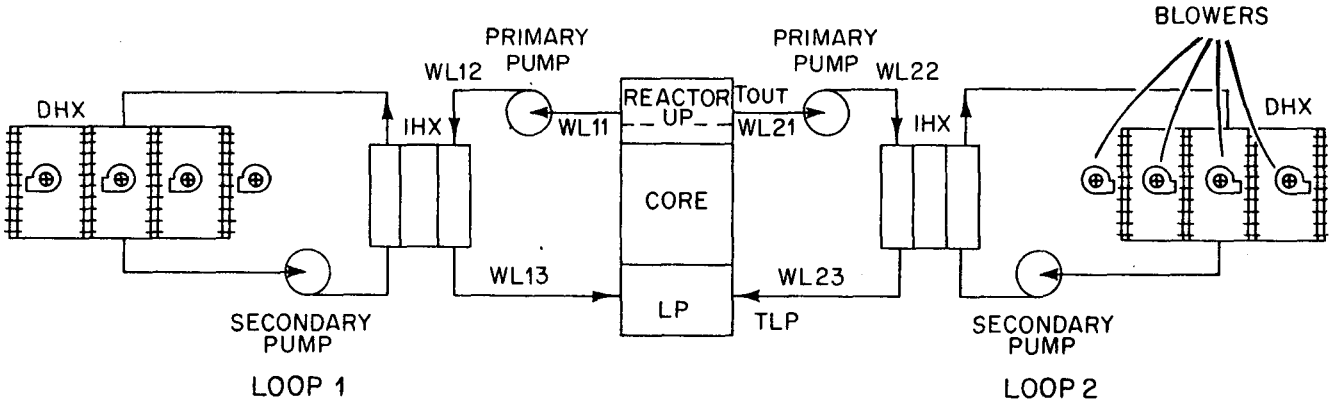

Fig. 1.2 Simplified Diagram of FFTF

For the case of the FFTF model with the new pump model, results of a two-loop simulation with a 10 percent set point change in the primary pump speed for one loop while the second loop pump speed is unchanged will be presented.

1.2 A Brief Literature Review

If the possible operating conditions of hydraulic-turbine and centrifugal-pump installations are compared, it soon becomes apparent that the pumps are subject to much wider and more involved variations than are the turbines, especially during the transient states of starting, stopping, or emergency operation. In turbines the direction of flow and the direction of rotation are always the same, even in case of a breakdown of the machine itself or trouble in the penstock and auxiliary equipment. Thus the machine performance always lies in the quadrant of normal turbine operation, and since the hydraulic characteristics are very well-known in this quadrant, it is a comparatively straightforward matter to predict the complete performance during any possible transient condition. On the other hand, under similar conditions with a pump installation, the flow can completely reverse direction as can the rotation. The machine in this case ceases to be a pump and, after passing through a zone of energy dissipation, becomes a runaway turbine. This great variation in performance gives rise to many questions such as the runaway speed of the machine as a turbine, the time of reversal, the magnitude of the accelerating forces, the effect on the surge cycle in the discharge line, the maximum and terminal reverse rates of flow, etc. Unfortunately these questions are very

difficult to answer, because, although the hydraulic performance of the machine is well-known as long as it is acting as a pump, comparatively little study has ever been made of the performance as an energy dissipator or as a turbine.

Professor Hollander of the California Institute of Technology in 1931 furnished the basic test data of a pump in what is known as the Karman-Knapp circle diagram (Donsky, 1967). The testing procedure used to obtain those data can be found in an article by Mr. Swanson (Stepanoff, 1957). All the test data were presented in percentages of the head, flow, torque, and speed values at the best efficiency point. This makes the developed characteristics applicable for all pumps having approximately the same specific speed. By the use of the homologous laws for pumps (Parmakian, 1955; Mead, 1933) the test data were extended into families of head and torque curves in a convenient manner to obtain families of dimensionless head-discharge curves in a single diagram and to form complete pump characteristics. His study furnished most of the background for all the subsequent work.

Instead of obtaining the head-discharge curve from Karman-Knapp diagrams at every point on the regime of operations as Professor Hollander did, Streeter (1967) in his discussion assumes a general polynomial relationship for the head-discharge curve and fits the polynomial at fewer points in each regime. However, he assumed a second order polynomial which is less accurate for a wide range of the pump operation.

A more convenient approach which also avoids table look-ups during computation has been discussed by Madni and Cazzoli (1978) in

their BNL-NUREG-50859 report. They assumed polynomial relations up to fifth order and fitted the data points from Streeter. By this, the coefficients of the assumed polynomial at each operational regime in the complete characteristics were obtained and used for further simulation. This has been adopted in the present work also.

In a more recent work by Wylie and Streeter (1967), the so-called Suter definition is used. The advantage of using this procedure is that only two continuous curves are needed. However, the disadvantage is that the resulting curves are difficult if not impossible to interpret from a physical standpoint.

CHAPTER 2

PUMP MODEL

2.1 Four Quadrant Pump Operation

In a severe accident such as a sudden power failure, the pump can go through several regimes of operation. This is illustrated in Figure 2.1. In the initial stages of the transient, with positive rotational speed and positive discharge, the pump is operating in the zone of normal operation. As flow and pumping head are reduced, negative pressure waves propagate downstream in the discharge line, and positive pressure waves propagate upstream in the suction line. Flow in the discharge line decreases rapidly to zero and then reverses in the loop; the pump enters the zone of energy dissipation, until pump speed also reverses. With both flow and speed becoming negative, the pump is in the zone of turbine operation. Much later, if the pump flow recovers and become positive again, the pump enters the zone of reverse pump operation. Pump performance curves involving all these regions of operation constitute the complete characteristics of the pump.

In order to avoid overlapping of curves, the complete characteristics are best presented as flow Q versus speed N (Karman-Knapp) diagrams in Figures 2.2 and 2.3. In Figure 2.2, the various zones of operation in four quadrants are shown. There are two zones of pump operation, the normal one and one in the second quadrant but with reverse rotation, head and flow being in the direction same as in normal pumping. Likewise, there are two zones of turbine operation, the normal

$\nu = Q/Q_R$

$\alpha = \Omega/\Omega_R$

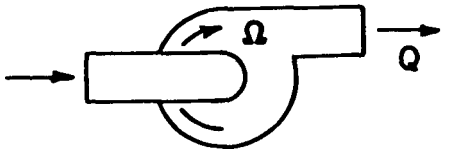

NORMAL PUMP
$(+\nu, +\alpha)$

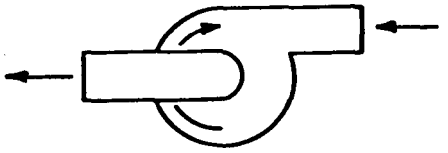

ENERGY DISSIP.
$(-\nu, +\alpha)$

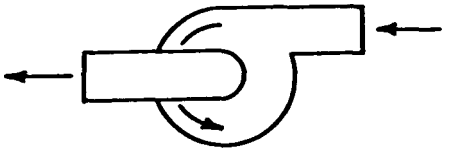

NORMAL TURBINE
$(-\nu, -\alpha)$

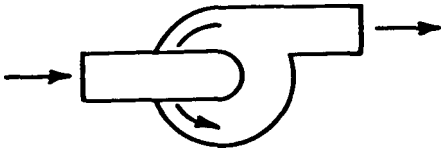

REVERSE PUMP
$(+\nu, -\alpha)$

Fig. 2.1 Pump Configurations under Different Regimes of Operation

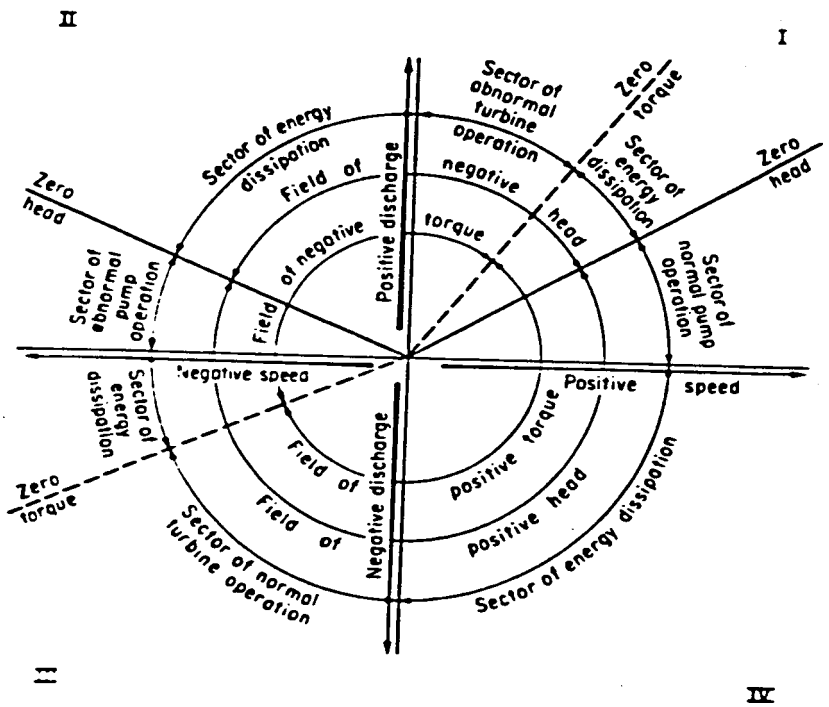

Fig. 2.2 Explanatory Chart for Complete Characteristics Diagram. -- (From Knapp, 1937)

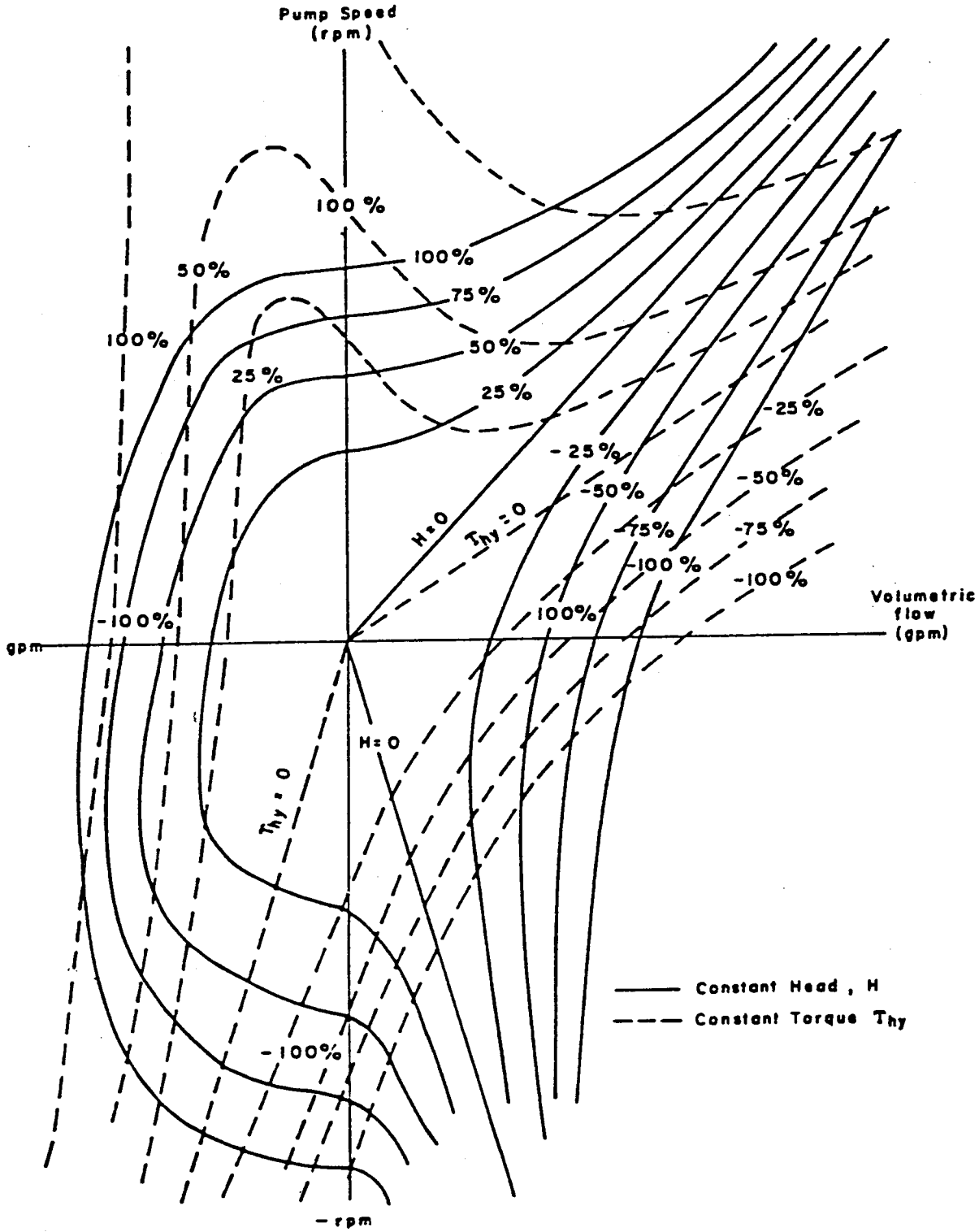

Fig. 2.3 Four-Quadrant Pump Characteristics Curves. -- (From EPRI NP-408, 1977)

one is the third quadrant and the abnormal or outward-flow one in the first quadrant. In between there are zones of energy dissipation in which no useful work is done either on or by the fluid. For example, the entire fourth quadrant is such a zone; at positive speed and head there is reverse flow through the machine, against its pumping action.

2.2 Non-dimensional Homologous Model

Single-phase pump performance is generally measured and described in terms of head and torque for a given speed, flow rate and fluid density. These are the pump characteristic parameters. For a proper simulation of the pump behavior, we need values of these parameters for all regions of interest, and for the full-scale pump in question. However, pump manufacturers generally supply performance data of their units for normal operation only, and little data are available for either the zone of energy dissipation or the zone of turbine operation. Due to practical limitations, most additional data available is from scaled-down models, not necessarily with liquid metal, and from selected combinations of operating conditions within the capabilities of the test facility. Hence, to obtain the complete characteristics, one can use homologous theory (Streeter and Wylie, 1967), which enables the use of results of model tests with similar pumps, and also extends the selected results to cover all possible combinations of pump parameters. When two pumps are geometrically similar, and have similar streamline patterns of flow through them, they satisfy the conditions for dynamic similarity (except for viscous effects). In terms of head H, discharge Q, diameter D, and rotational speed N, the homologous conditions are given by:

$$\frac{H}{N^2D^2} = \text{constant}; \quad \frac{Q}{ND^3} = \text{constant} \tag{2.2.1}$$

In other words, these ratios must be the same for any of the homologous series of units when they are operating in a dynamically similar manner. When studying transient effects in a given pump whose diameter is fixed and known, one may absorb D in the constant; hence

$$\frac{H}{N^2} = \text{constant}; \quad \frac{Q}{N} = \text{constant} \tag{2.2.2}$$

The parameter defining the similarity is the specific speed, defined as

$$N_s = \frac{N\sqrt{Q}}{H^{3/4}} \tag{2.2.3}$$

If the pump parameters are non-dimensionalized through division by the appropriate rated values, then the non-dimensional (homologous) characteristics of the pump are independent of the liquid pumped, and the shape of the characteristic curve then depends on the rated specific speed (Donsky, 1967; Stepanoff, 1957). This assumes negligible viscosity effects. In general, the influence of viscosity and other scale effects on pump head and torque is small for single-phase flow (Runstadler, 1976).

If pump head, torque, flow rate and speed are divided by their respective rated values, the dimensionless parameters are written as follows:

$$h = H/H_R$$

$$\beta = \tau_{hyd}/\tau_R$$

$$\nu = Q/Q_R$$

$$\alpha = N/N_R \qquad (2.2.4)$$

On the basis of Equation 2.2.4, Equation 2.2.2 may be rewritten to get the dimensionless-homologous relations

$$\frac{h}{\alpha^2} = \text{constant}$$

$$\frac{\nu}{\alpha} = \text{constant} \qquad (2.2.5)$$

Homologous head curves can be drawn by plotting

$$\frac{h}{\alpha^2} \text{ vs } \frac{\nu}{\alpha} \text{ in the range } 0 \leq \left|\frac{\nu}{\alpha}\right| \leq 1$$

and

$$\frac{h}{\nu^2} \text{ vs } \frac{\alpha}{\nu} \text{ in the range } 0 \leq \left|\frac{\alpha}{\nu}\right| \leq 1$$

Since both α and ν pass through zero during the course of a pump reversal, it is necessary to use both $\frac{h}{\alpha^2}$ vs $\frac{\nu}{\alpha}$ and $\frac{h}{\nu^2}$ vs $\frac{\alpha}{\nu}$ to avoid having the curves go to infinity.

Similarly, torque curves can be drawn by plotting:

$$\frac{\beta}{\alpha^2} \text{ vs } \frac{\nu}{\alpha} \text{ in the range } 0 \leq \left|\frac{\nu}{\alpha}\right| \leq 1$$

and

$$\frac{\beta}{\nu^2} \text{ vs } \frac{\alpha}{\nu} \text{ in the range } 0 \leq \left|\frac{\alpha}{\nu}\right| \leq 1$$

Figures 2.4 and 2.5 show these curves in all four quadrants and all regions of pump operation. Three letters are used for each curve segment; first: B or H to designate torque or head ratio, second: A or V to designate division by α^2 and ν^2, third: N, D, T or R to indicate normal, energy dissipation, turbine, or reverse pump operation zone. The curves can either be read in tabular form, or in the form of fitted polynomials. The fitted polynomial form approach was used in this analysis. The polynomial relations are of the following form:

$$\frac{\beta}{\alpha^2} \text{ or } \frac{h}{\alpha^2} = c_o + c_1 \frac{\nu}{\alpha} + c_2 \left(\frac{\nu}{\alpha}\right)^2 + \ldots\ldots + c_5 \left(\frac{\nu}{\alpha}\right)^5$$

$$\text{in the range } 0 \leq \left|\frac{\nu}{\alpha}\right| \leq 1 \qquad (2.2.6)$$

$$\frac{\beta}{\nu^2} \text{ or } \frac{h}{\nu^2} = c_o + c_1 \frac{\alpha}{\nu} + c_2 \left(\frac{\alpha}{\nu}\right)^2 + \ldots\ldots c_5 \left(\frac{\alpha}{\nu}\right)^5$$

$$\text{in the range } 0 \leq \left|\frac{\alpha}{\nu}\right| < 1 \qquad (2.2.7)$$

where c_o, c_1, ..., c_5 are constants for each polynomial. There are seven polynomials for head-discharge and seven for torque-discharge. The coefficients have been obtained by fitting the data points in Streeter and Wylie (1967) for all regions. A general approach for generating data points from a Karman-Knapp circle diagram is shown in reference Donsky (1967) and Knapp (1937). More details on pump coefficients are provided in Appendix A.

Once the characteristics are available in this fashion, the transient head H and torque T_{hyd} can be determined from rated values, operating speed and flow rate. The head then yields the pressure across the pump as

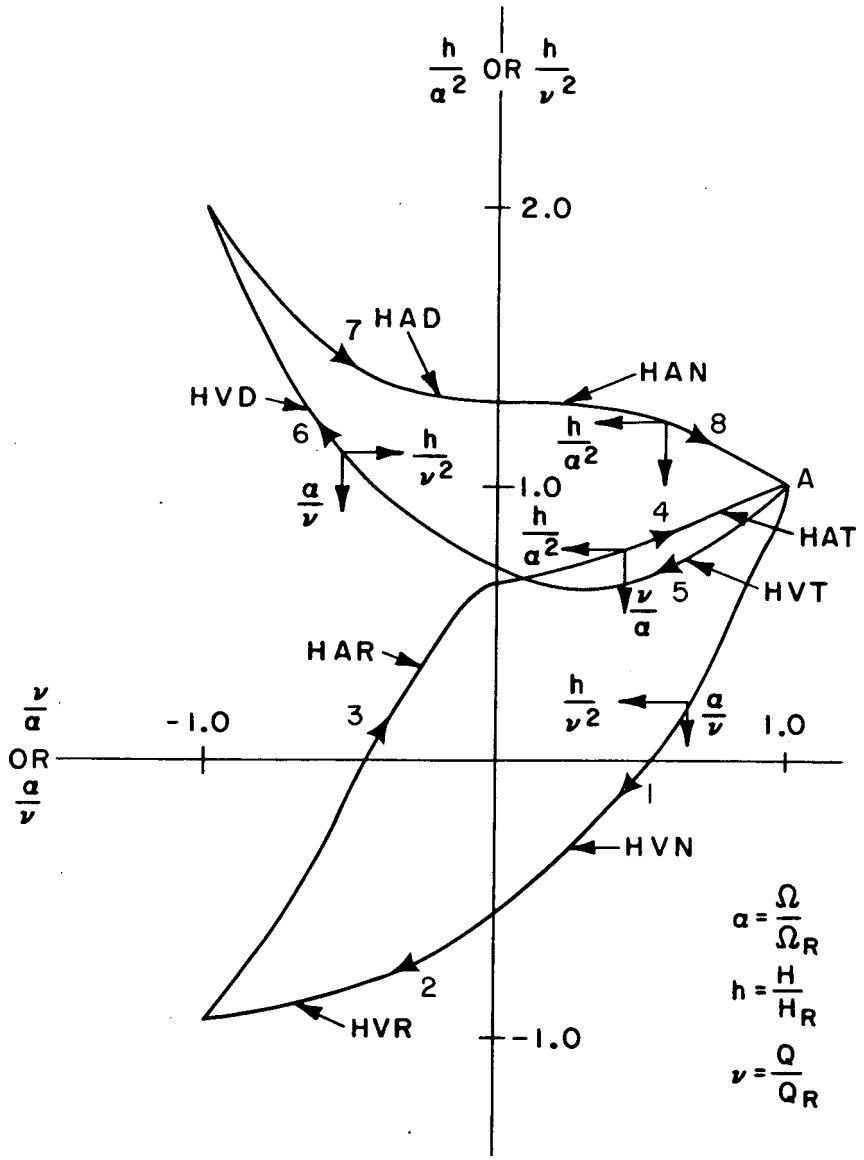

Fig. 2.4 Complete Homologous Head Curves

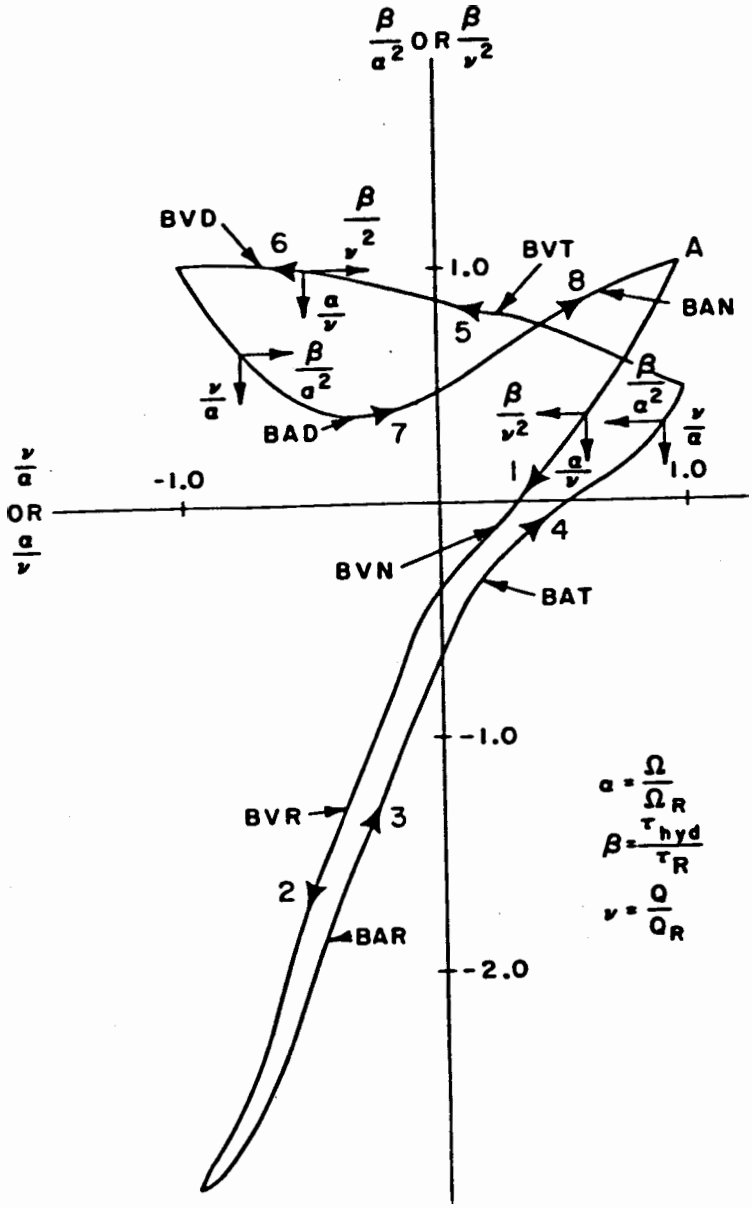

Fig. 2.5 Complete Homologous Torque Curves.

$$(P_{RISE})_{pump} = \rho_{in} (g/g_c) \text{ HOPP} \quad (2.2.8)$$

where ρ_{in} is the density of coolant at pump inlet.

2.3 Pump Speed Equation

At any time during a transient, the change in rotational speed of the pump is obtained from the application of angular momentum balance to the shaft and rotating assembly (including impeller, rotor, and flywheel).

The equation of motion is:

$$\frac{d\Omega}{dt} = \left(\frac{1}{I}\right) [\tau_m - \tau_{hyd} - \tau_{fr}] \quad (2.3.1)$$

where I is the moment of inertia of shaft, impeller and rotating elements inside the motor, τ_m is the applied motor torque (set to zero during coastdown), τ_{hyd} is the hydraulic load torque due to fluid at the impeller, τ_{fr} is the frictional torque, and Ω is the angular speed of the pump (rad/s).

With the design speed in rpm, the equation can be rewritten as

$$\frac{dN}{dt} = \left(\frac{60/2\pi}{I}\right) [\tau_m - \tau_{hyd} - \tau_{fr}] \quad (2.3.2)$$

The moment of inertia I has a strong influence on the rate of pump coastdown. The hydraulic torque is obtained from pump characteristics. Frictional torque (due to bearing losses, fluid friction, etc.), becomes important at low pump speeds, such as occurs in the pump coastdown to natural circulation transient.

2.4 Pump Friction

Torque due to friction losses in the pump is represented in the model as a polynomial of the form:

$$\tau_{fr} = \tau_R \ (c_o + c_1\alpha + c_2 \alpha|\alpha|) \qquad (2.4.1)$$

where τ_R is the rated hydraulic torque and α is the normalized pump speed. The pump vendor data for CRBRP pumps (Batenburg, 1978) is used to provide the coefficients.

The coefficients in Equation 2.4.1 are:

$$c_o = 0.012, \quad c_1 = 0.23, \quad c_2 = 0.0$$

$$\text{for } \alpha > 0.0117$$

$$c_o = 0.117, \quad c_1 = 8.97, \quad c_2 = 0.0$$

$$\text{for } 0.005 \leq \alpha \leq 0.0117 \qquad (2.4.2)$$

However, for very low speeds (approaching locked rotor), unrealistically high values of τ_{fr} are obtained, so a third region is defined where

$$c_o = 0.0 \quad c_1 = 14.77, \quad c_2 = 0.0$$

$$0 \leq \alpha \leq 0.005 \qquad (2.4.3)$$

This gives the correct limit for $\alpha = 0$, and removes any instabilities that would otherwise be caused in the hydraulic transient.

The constants in the BRENDA pump model have also been used for the FFTF because both pumps have approximately the same speed (1170, 1110 rpm for BRENDA and FFTF respectively).

2.5 CRBR Flow Rate Equation

The complete derivation of the flow momentum balance equation for the primary loop is given in the report NUREG-0110 by Shinaishin (1976). We will only briefly review this equation here.

A momentum balance equation is integrated over the length of each region in each loop (Figure 1.1) to yield an equation of the form:

$$\frac{L}{A}\frac{d\bar{W}}{dt} + \Delta\ (W^2/\rho_L A^2) = \Delta P + \Delta\ (\rho_L g Y) - \text{Losses} \qquad (2.5.1)$$

Applying the above equation to CRBR, an overall momentum balance in the primary loop leads to the following equation (section A-6.5 of Shinaishin, 1976):

$$\frac{dW_{ps}}{dt} = \left(\frac{1}{\tau_{wp}}\right)[15.839\rho_{NA}\ (T_{p7}) - 11\rho_{NA}\ (T_{p1}) - 3\rho_{NA}\ (\bar{T}_{p1}) -$$
$$- 5.68\rho_{NA}\ (T_{p3}) + (HOPP - 21.4)\ \rho_{NA}\ (T_{p4}) +$$
$$+ 25.37\rho_{NA}(\bar{T}_{p5}) - \{f_{p1}/N_L^2 + f_{143}\ (FFC/N_{SUB})^2 + f_{p2}\}\ W_{pS}^2] \qquad (2.5.2)$$

in which

HOPP = head of primary pump

$$\tau_{wp} = \frac{3.55}{N_L} + \frac{6.55}{N_{SUB}} \cdot FFC \qquad (2.5.3)$$

where FFC is the fraction of sodium passing through core, N_{SUB} is the number of fuel subassemblies in the core and f_{p1}, f_{143} and f_{p2} are constants determined from the initial steady state values of the pressure and temperature in the loop. The main assumptions made are that the sodium levels in both the reactor outlet plenum and the primary pump tank are fixed and that the gas pressure above the sodium

surface is constant. It was also assumed that the losses (mainly due to friction) in any region are proportional to the square of the flow in that region.

2.6 FFTF Flow Rate Equation

The hydraulic flow equation for the FFTF is given in general by Addition et al. (1976, p. 31):

$$PI = PG + PH + PN - PF \qquad (2.5.4)$$

PI = Fluid inertial pressure

$$= \frac{\partial W_i}{\partial t} \frac{1}{g_c} \sum_j \frac{L_j}{X_j}$$

where W_i = Mass flow rate in loop segment i

t = Time

g_c = 32.179 (lb_m/lb_f) (ft/sec^2)

L_j = Length of subsection j, having uniform cross section X_j, in flow loop i

X_j = Cross sectional flow area of flow loop section i, subsection j

PG = Net cover gas pressure for flow loops that contain primary fluid-free levels

PH = Pump head (pressure change through the pump)

PN = Pressure change in flow loop due to natural circulation effects

$$= \sum_{k=1}^{i} (\rho_k)(h_k),$$ (summation is performed over all vertical segments in the plant for each flow loop

ρ_k = Fluid density in vertical segment k

h_k = Vertical height of segment k

PF = Friction and turbulent pressure losses in flow loop in each segment

Referring to Figure 1.2, the momentum equation for the flow rate WL1(1), WL1(2), or WL1(3), where WL1(1), WL1(2), and WL1(3) represent respectively the flow rate between the reactor outlet and pump inlet, pump inlet and IHX, and the IHX and reactor inlet is given by:

$$\frac{d}{dt} WL1(I) = AOL1(I)[PIN1(I) - POUT1(I) - RHOL1(I) \times G \times YL1(I) + REST1(I)] \quad (2.5.5)$$

$$REST1(I) = (WL1B(I)/PAL1(I))^2 \times \left(\frac{1}{ROIN1(I)} - \frac{1}{ROUT1(I)} - FL1(I) \times PAL1(I)^2\right) \quad (2.5.6)$$

$$PAL1(I) = \pi \times (R1(I))^2 \quad (2.5.7)$$

$$PIN1(2) = POUT1(1) + PUMP(1) \quad (2.5.8)$$

where

I = 1, 2, 3

R1(I) = Radius of pipe in flow loop section I

YL1(I) = Vertical height of section I

AOL1(I) = Area over length of flow loop section I

ROIN1(I), ROUT1(I) are the inlet and outlet densities at flow section I

PIN1(I), POUT1(I) are the inlet and outlet pressures at flow section I

WL1B(I) = Initial flow rate at flow section I

FL1(I) = Frictional losses in section I

G = g_c = 32.179 (lb_m/lb_f) (ft/sec^2).

A similar flow rate equation was also written for the second loop. The complete set of equations with the assumptions for the FFTF has been obtained from Sands (1980).

2.7 Flow Chart For Simulation of Homologous Characteristics of a Pump

Figure 2.6 shows a flow chart diagram for implementing homologous characteristics of a pump. Since pump failure can occur at any point in the operational regime, it is necessary to write a general simulation flow chart that can be used to simulate and calculate the transient head HOPP and torque τ_{hyd} which are to be used in equations 2.5.2 and 2.3.1 from the homologous characteristics, knowing rated value, operating speed and flowrate. In implementing the flow chart, it was assumed that a transient will start from the normal operation regime of the pump and at point A of Figure 2.2.1. The transient causes this point A to move on the characteristic curve. Thus, depending on the new value of α/ν (i.e., less than or greater than one), the path of A could be either along HVN, HVR, HAR, HAT, HVT, HVD, HAD and HAN or along HAN, HAD, HVD, HVT, HAT, HAR, HVR and HVN respectively as given below.

In sketching the flow chart which takes these two cases into consideration, indices 1-8 representing points on HVN, HVR, ..., HAD and HAN respectively were established. Initially, α/ν and the index were set equal to 1 to calculate HVN. With the initiation of the transient, the flow WPS and the speed ENPP could change and are governed by equations 2.5.2, 2.3.1 and 2.2.7, so α/ν is calculated to establish the path of the point A. The value of α/ν is checked and if it lies

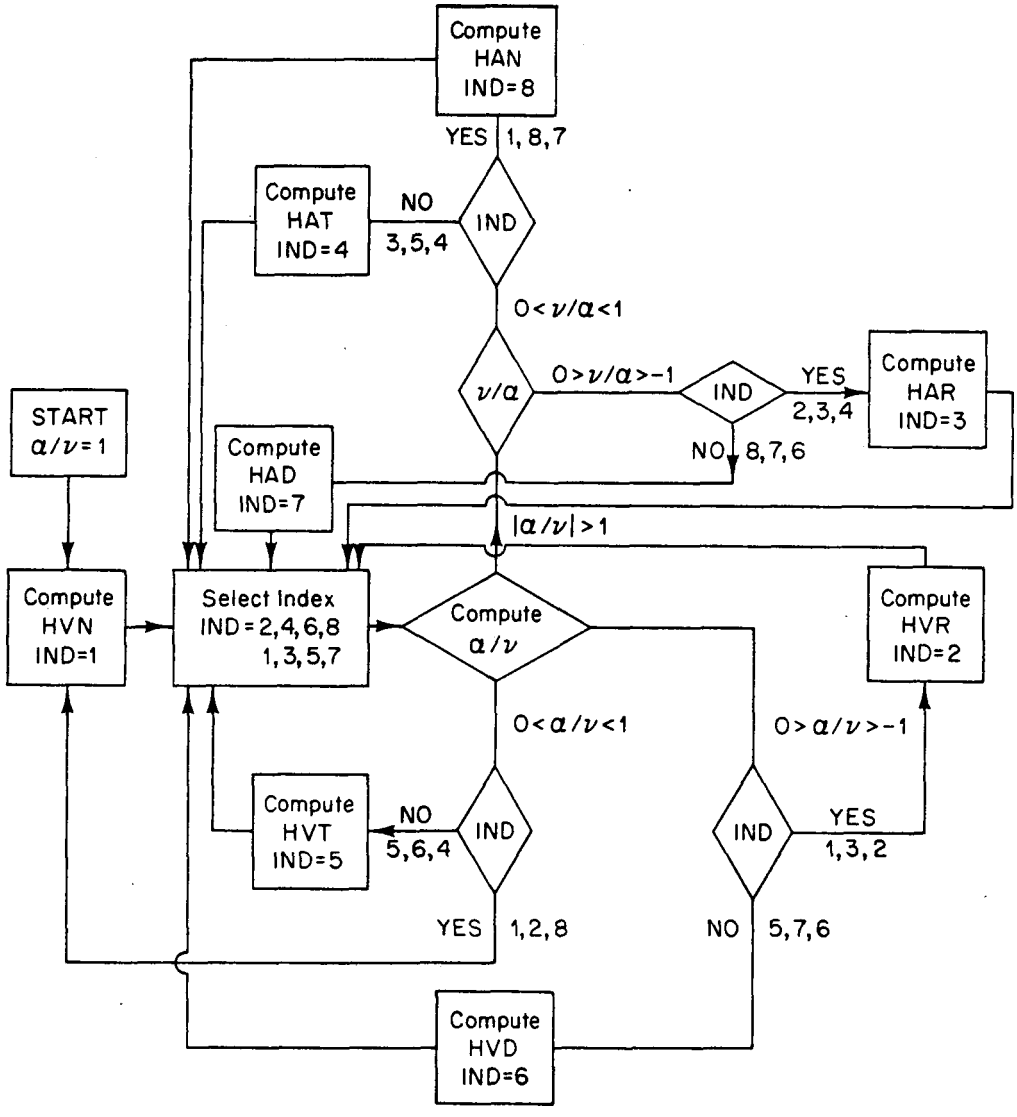

Fig. 2.6 Flow Chart for Implementing Homologous Characteristics of a Pump

between 0 and 1, and the previous value of the index is 1, HOPP is calculated using HVN and the point will still be on index 1. If, however, α/ν is such that the point A has moved on to either HVR, HVT, or HAN, then HOPP is calculated correspondingly and the index is set to either 2, 5 or 8. This process is repeated to track the path of A throughout the transient. This flow chart has been implemented in FORTRAN IV as a part of BRENDA.

CHAPTER 3

RESULTS

3.1 Initial Results with Pump Alone

To test the pump model separately, the pump coastdown to its natural circulations was carried out. For this test case, the applied motor torque, τ_m, was set to zero at time t = 0. Following loss of the motor torque, the pump starts coasting down, causing the head across the impeller and the sodium flow rate to decrease. Figures 3.1, 3.2, and 3.3 compare the predicted pump speed, flow and head transients resulting from such an accident to those of (Madni and Cazzoli, 1978).

Coastdown of pump speed is illustrated in Figure 3.1. The curve shows a slight dip, at about 40 seconds, indicating a more rapid rate of speed decay. This is due to the increased frictional losses under low speed and flow conditions. The pump flow rate decays similarly to the speed, but instead of dropping to zero, it settles down to a small value, Figure 3.2. Pump head, on the other hand, drops very rapidly in the first few seconds of the transient, and with pump speed approaching zero, it becomes slightly negative, representing the pump condition as a resistance to flow in the circuit. This is not evident in Fiugre 3.3 due to its scale. The transient operating points of the impeller are shown plotted on its homologous head characteristics in Figure 3.4. Here, the condition of negative head is very clearly evident for t > 38 secs.

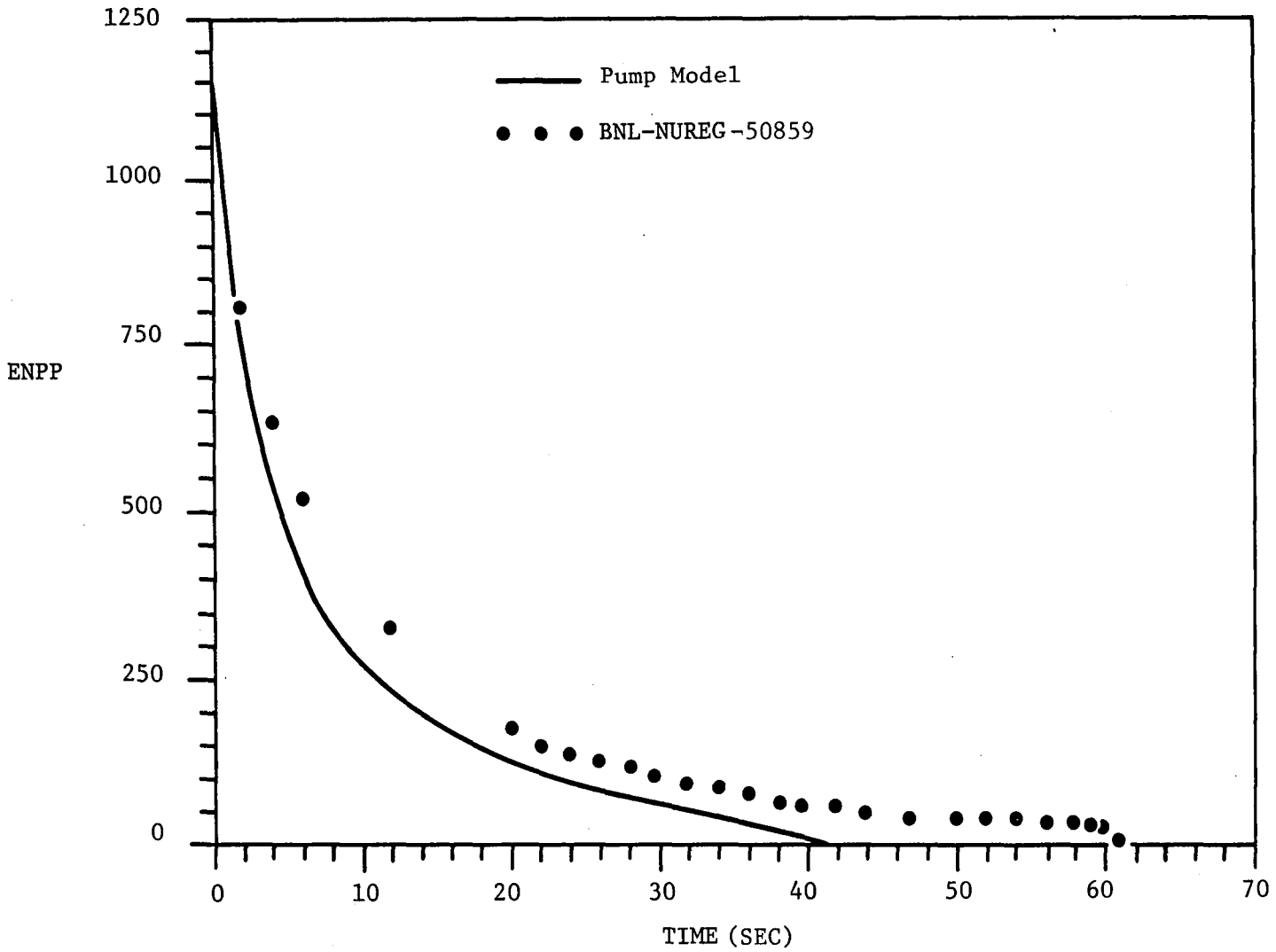

Fig. 3.1 Computed Primary Pump Speed Decay.

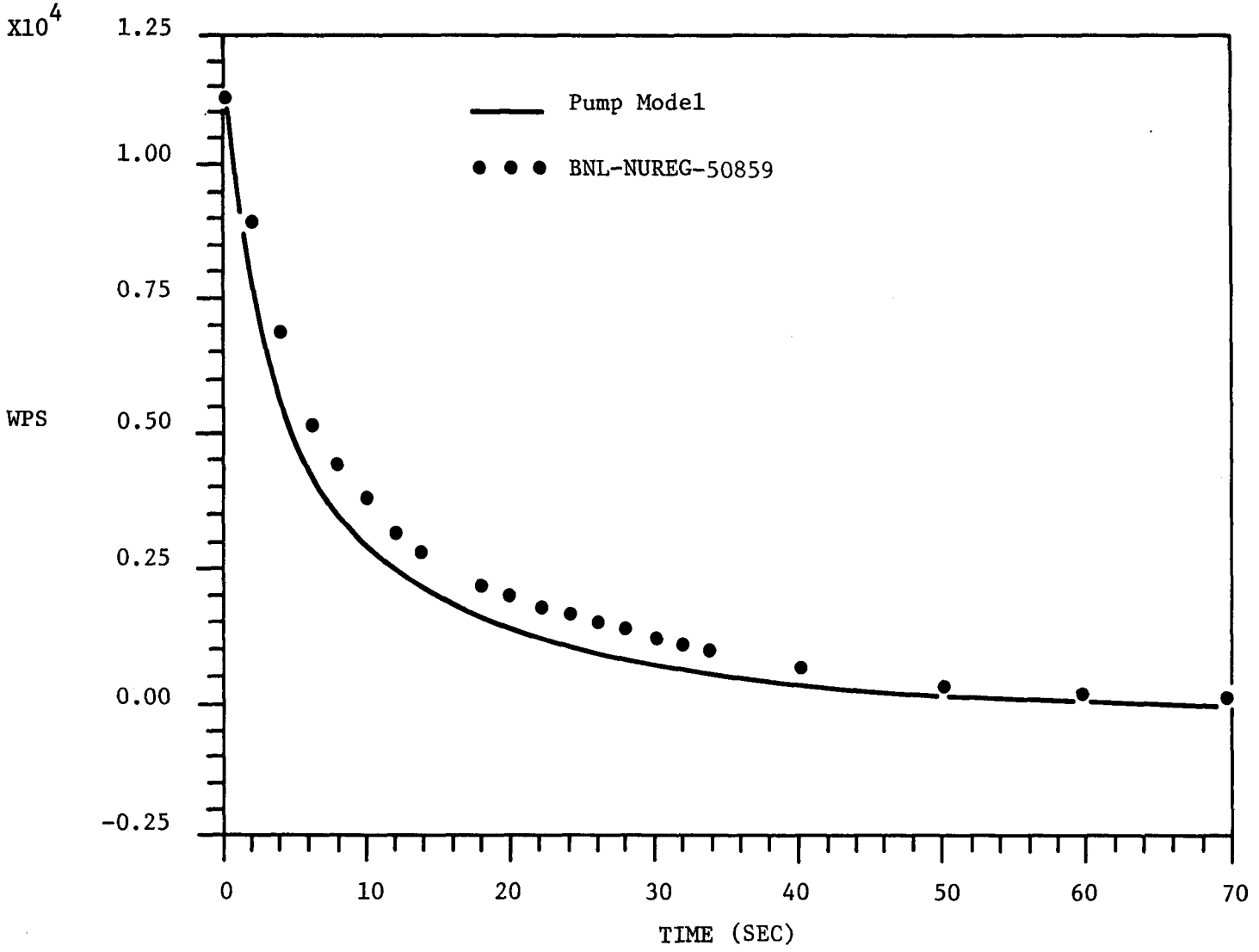

Fig. 3.2 Computed Flow Rate Decay.

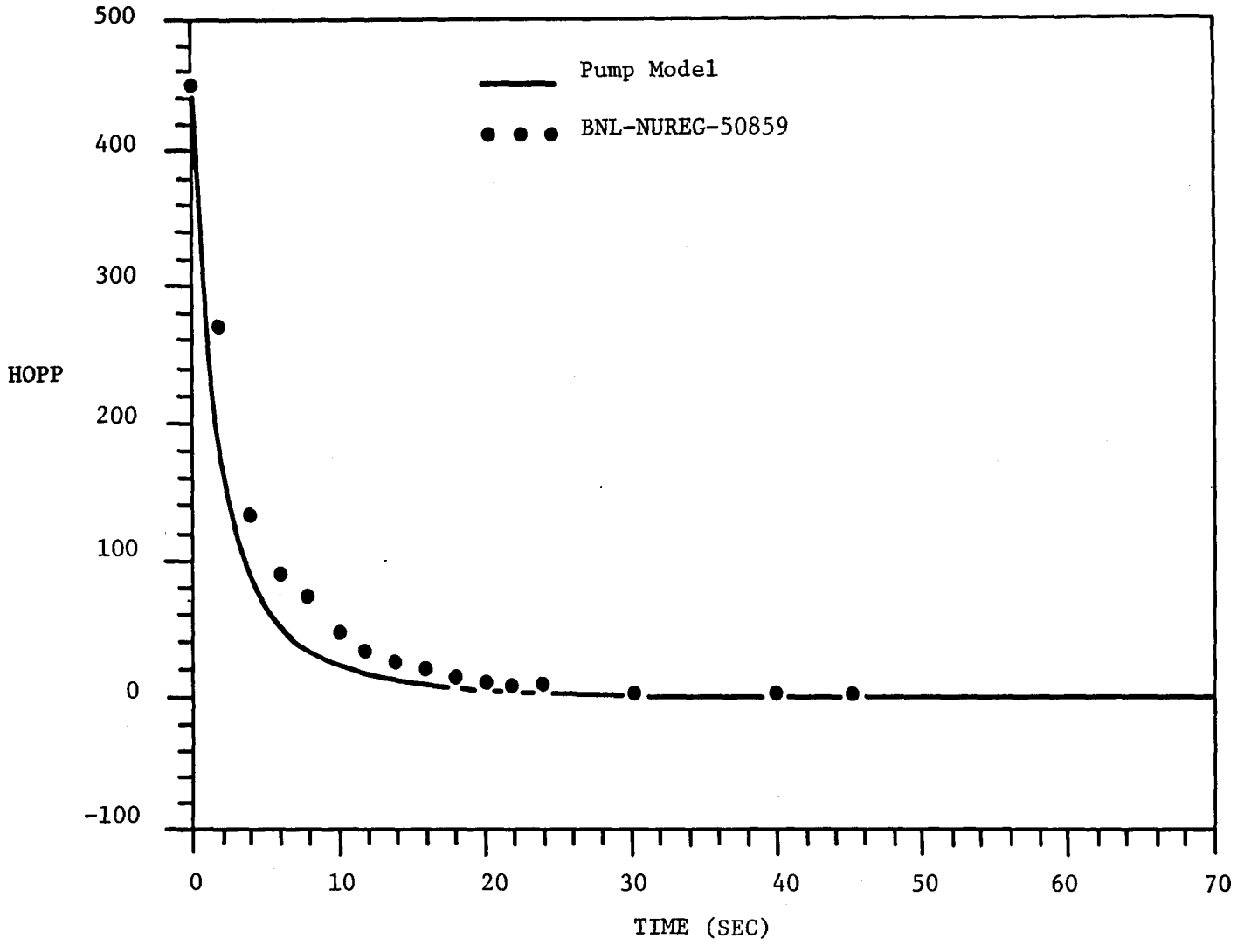

Fig. 3.3 Computed Decay of Primary Pump Head.

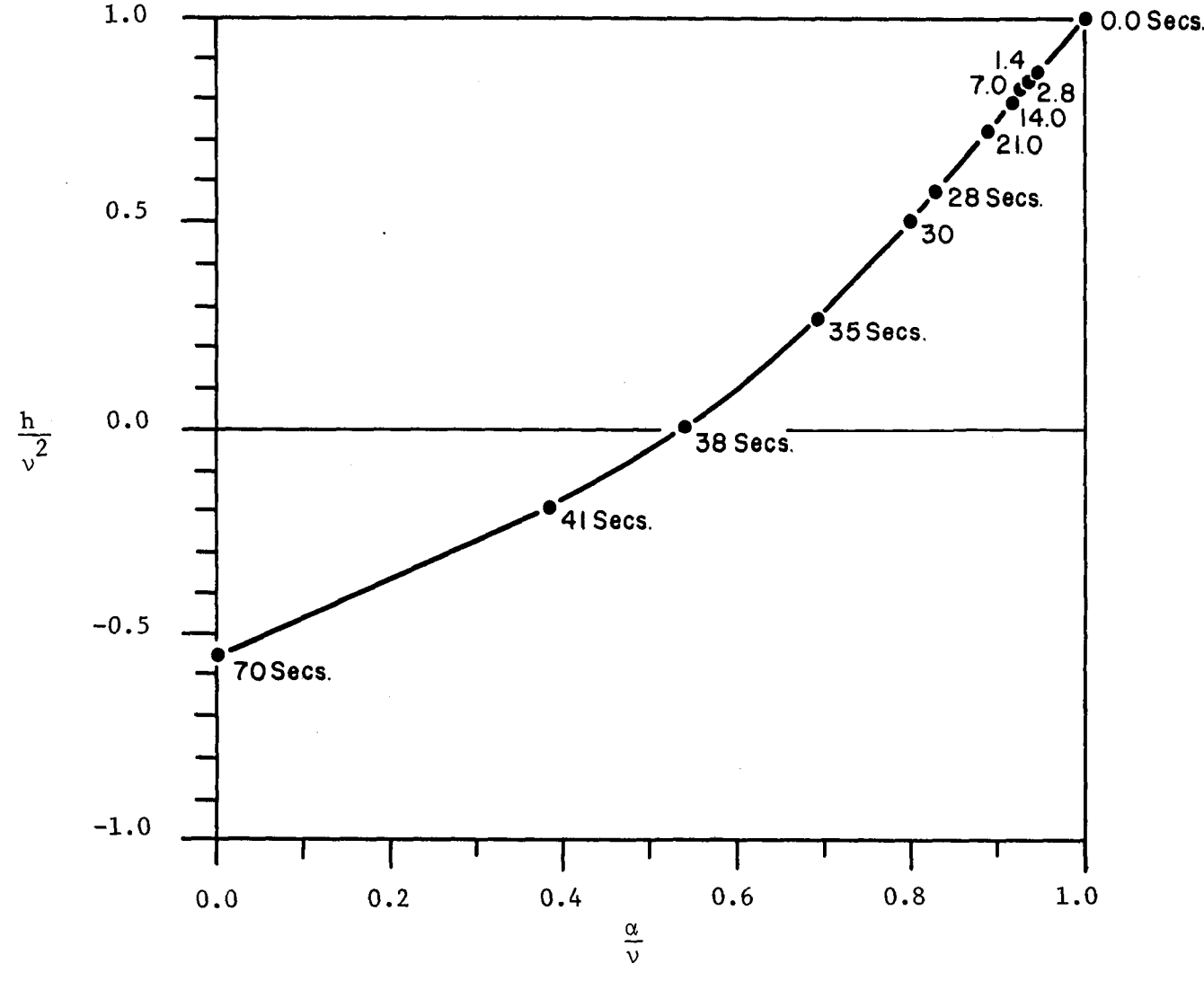

Fig. 3.4 Transient Operating Points on Pump Head Curve

3.2 System Transient with Pump Model Coupled to BRENDA

To test the pump model with the rest of the system, the old pump which has been represented in tabular form in BRENDA was replaced with the new pump model, and a one-loop simulation of the three-loop plant was performed. The following transients were conducted.

1. Primary pump coastdown to natural circulation.
2. A deviation of the primary pump speed from a set point (10 percent decrease of primary speed) with the plant controllers being operative.

Results obtained from such transients are illustrated in Figures 3.5 and 3.6. Figure 3.5 illustrates the primary pump coastdown to natural circulation. The primary speed ENPP goes to zero while the flow rate WP although decaying similarly to the speed, settles down to a small value of about 1/20 of its steady state value (i.e., to its natural circulation value). The pump head HOPP, on the other hand, drops very rapidly in the first few seconds of the transient. The primary coolant exit temperature TP3 rises to about 5000°F (no boiling is provided in the model) and the average fuel temperature TAF reaches about 3500°F (no fuel melting is included). Both the intermediate speed ENIP and the flow rate WI also decrease but less severely. It may be concluded that within 10 seconds the sodium would have reached boiling and some fuel would reach melting if no scram takes place. Figure 3.5 also includes other variables from the secondary loop, recirculating loop, and the tertiary loop, but these transients have not

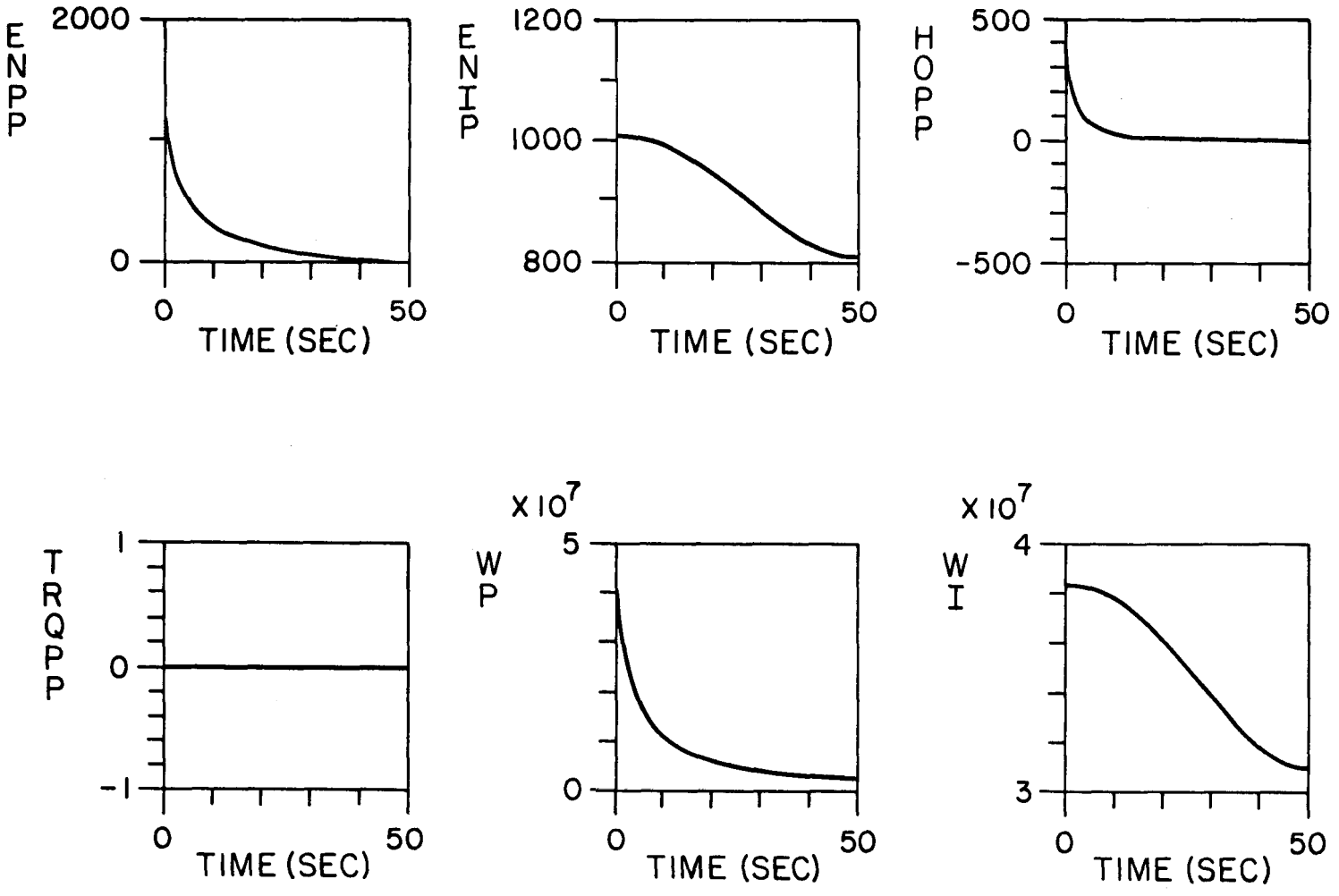

Fig. 3.5 Coastdown Characteristics - BRENDA

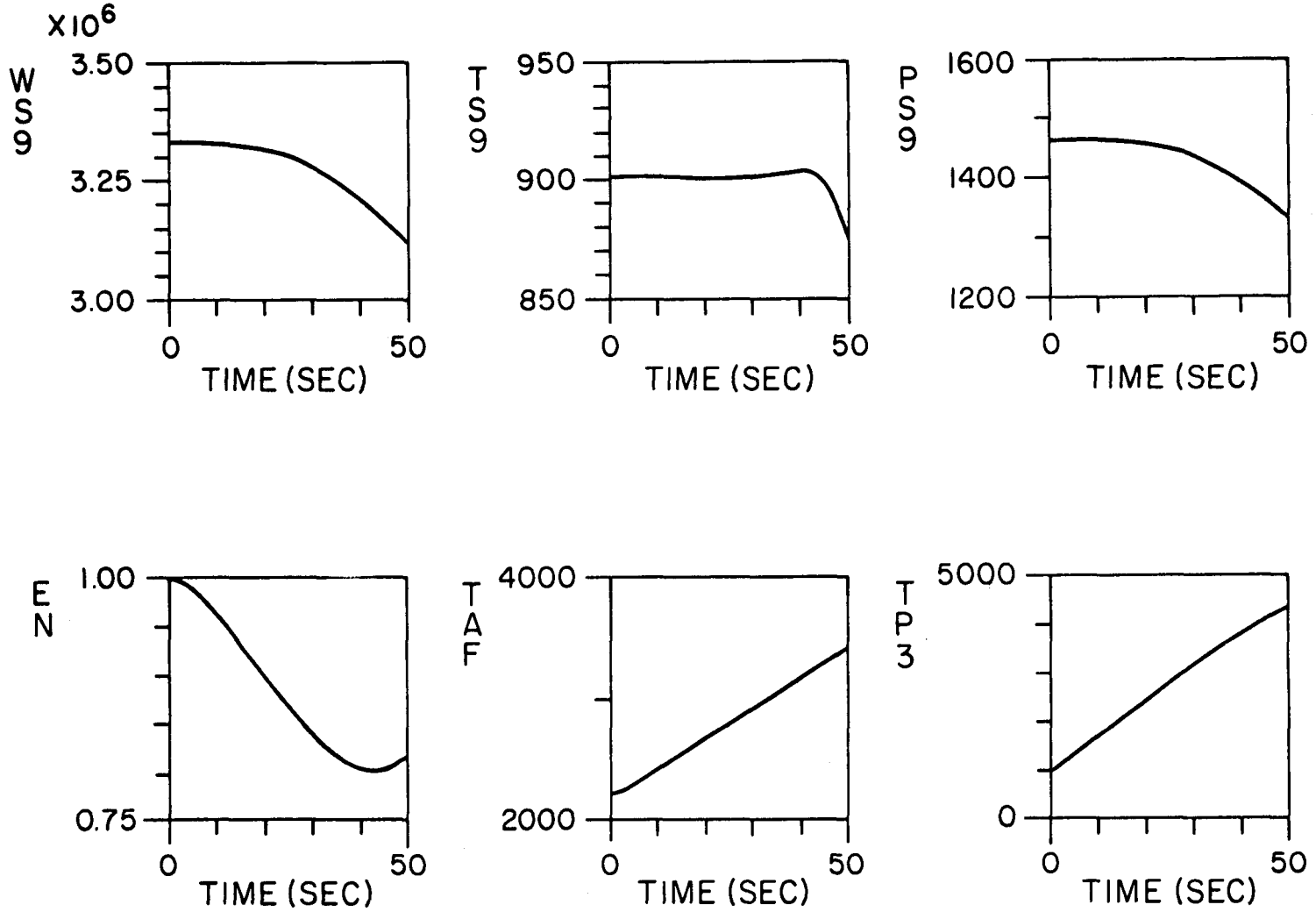

Fig. 3.5 -- Continued Coastdown Characteristics - BRENDA

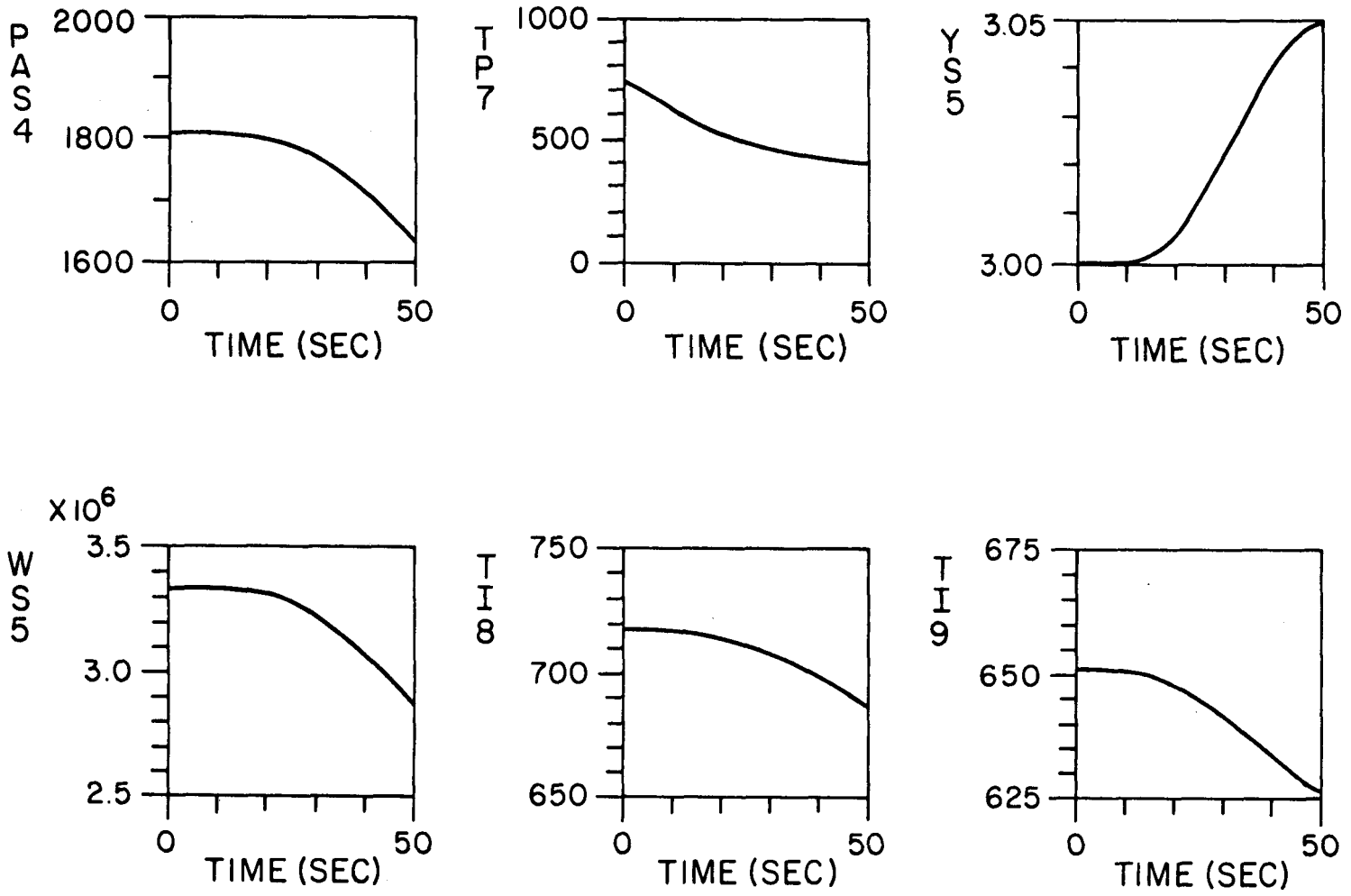

Fig. 3.5 -- Continued Coastdown Characteristics - BRENDA

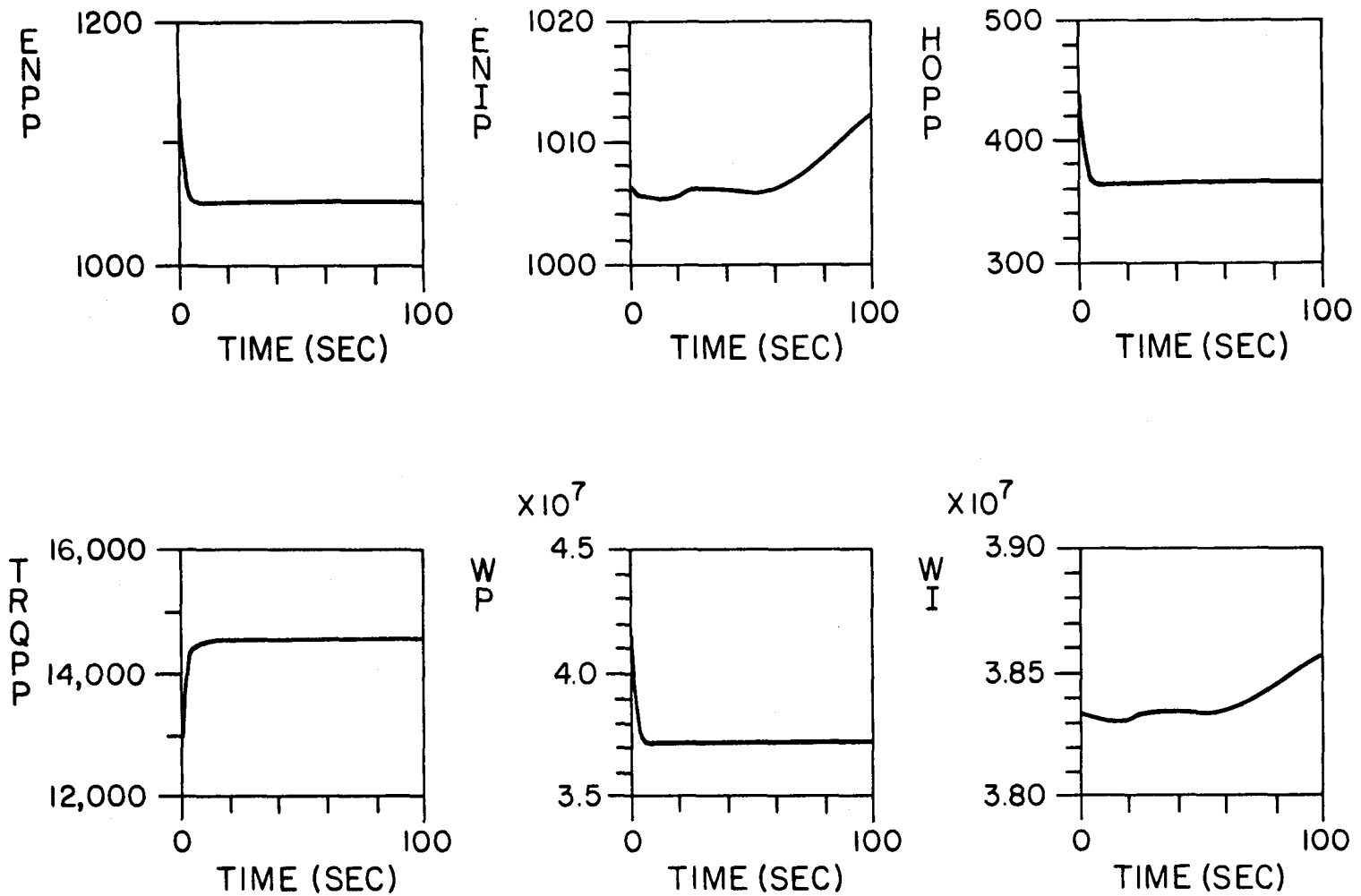

Fig. 3.6 10 Percent Deviation of Primary Speed - BRENDA

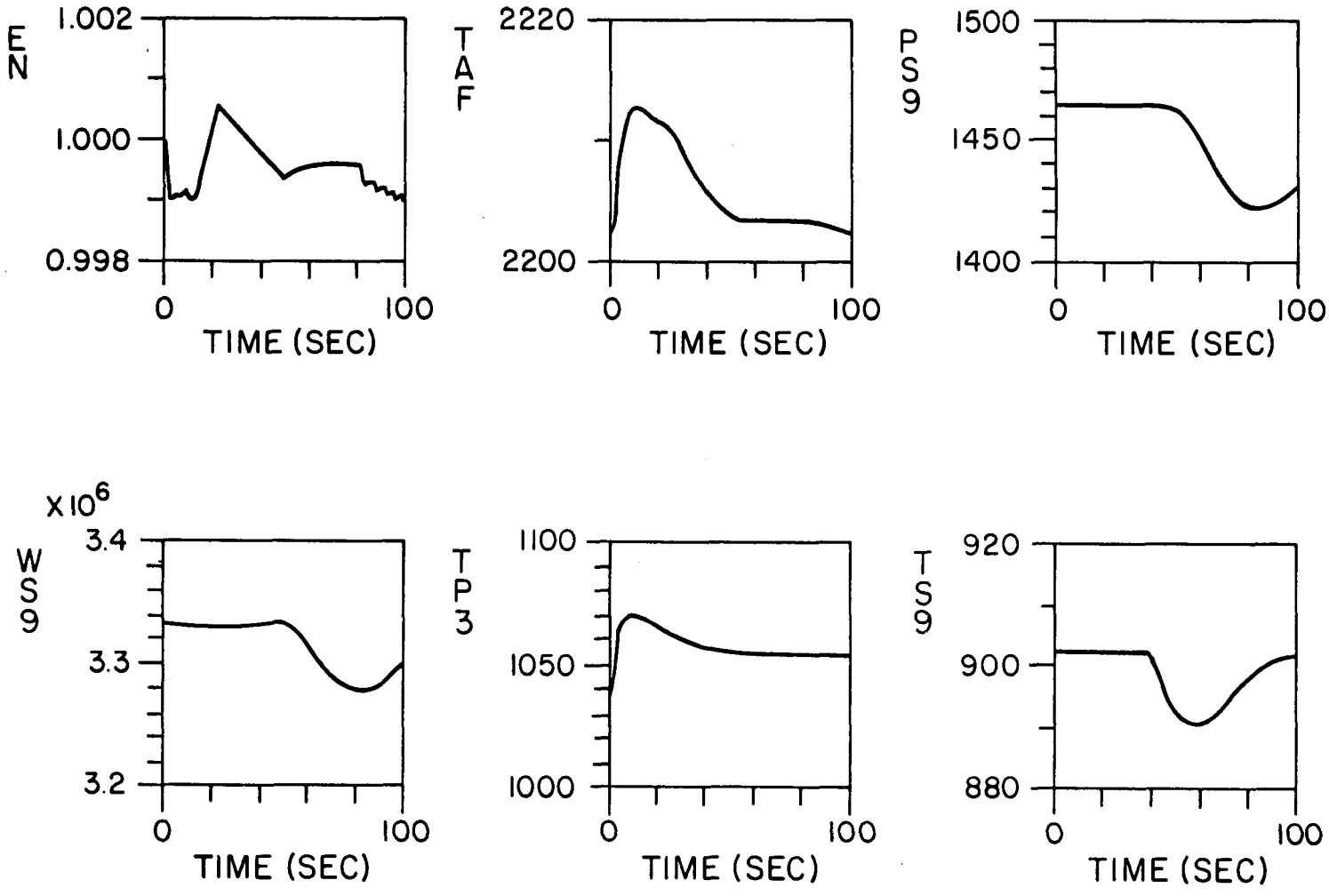

Fig. 3.6 -- Continued 10 Percent Deviation of Primary Speed - BRENDA

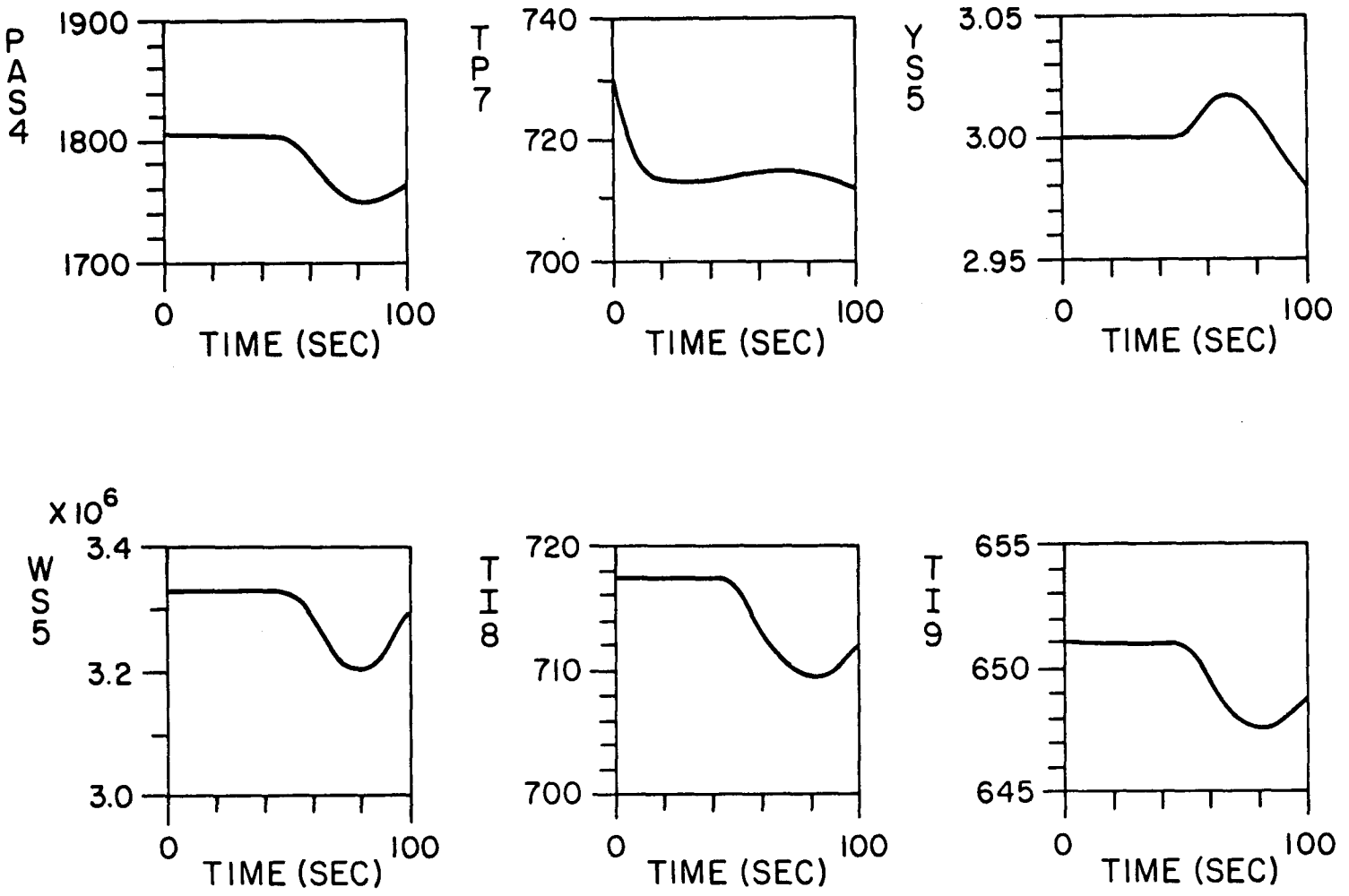

Fig. 3.6 -- Continued 10 Percent Deviation of Primary Speed - BRENDA

been felt as severely as in the primary loop during the first 50 seconds of the transient.

The controlled plant transient following a 10 percent decrease of primary speed is shown in Figure 3.6. The primary speed ENPP decreases very rapidly in the first few seconds and settles down to a steady value of about 1053 rpm as expected; this is the theoretical value for a 10 percent decrease from the steady state. The primary head HOPP and the loop flow rate WP also follow the same form as the speed ENPP. As both speed and flow rate decrease during the initial transient, the frictional torque on the system and hence the primary pump motor torque TRQPP increase until the system attains the new steady state value. The intermediate speed ENIP and the flow rate WI initially remain approximately constant due to time delays until about 50 seconds when the decrease of PS9 causes the error EPS9 to increase. This increase of EPS9 then causes both speed and flow to increase. The fuel average temperature in the core, TAF, and the core exit temperature, TP3, increase initially because of the initial decrease of flow rate. They all reach a new steady state. The reactor normalized power level, EN, remains approximately constant throughout the transient, although this is obscured by the scale used in the graph.

3.3 System Transient with Pump Model Coupled to FFTF

In this test, a two-loop simulation of the three-loop plant was performed. The two-loop simulation consisted of a single loop with one primary pump and a second loop representing two loops lumped together into one (Figure 1.2). A 10 percent decrease of the primary

speed ENPP of the single loop was postulated and the effect on the intact primary speed ENPP2 in the second loop was observed. The transients are shown in Figure 3.7.

The coastdown characteristics for this core were not investigated because the system thermal-hydraulics for the FFTF model did not include the secondary loop which is yet to be completed. This suggests that even though the results are qualitatively important, they need not represent the system response that would be obtained with complete model, both primary and secondary hydraulic model being included.

Looking at the characteristics, it is observed that the second loop with intact pumps experience transients that are less severe although generally similar in nature to the pump in the first loop with a 10 percent speed decrease. The transients are shown in Figure 3.7.

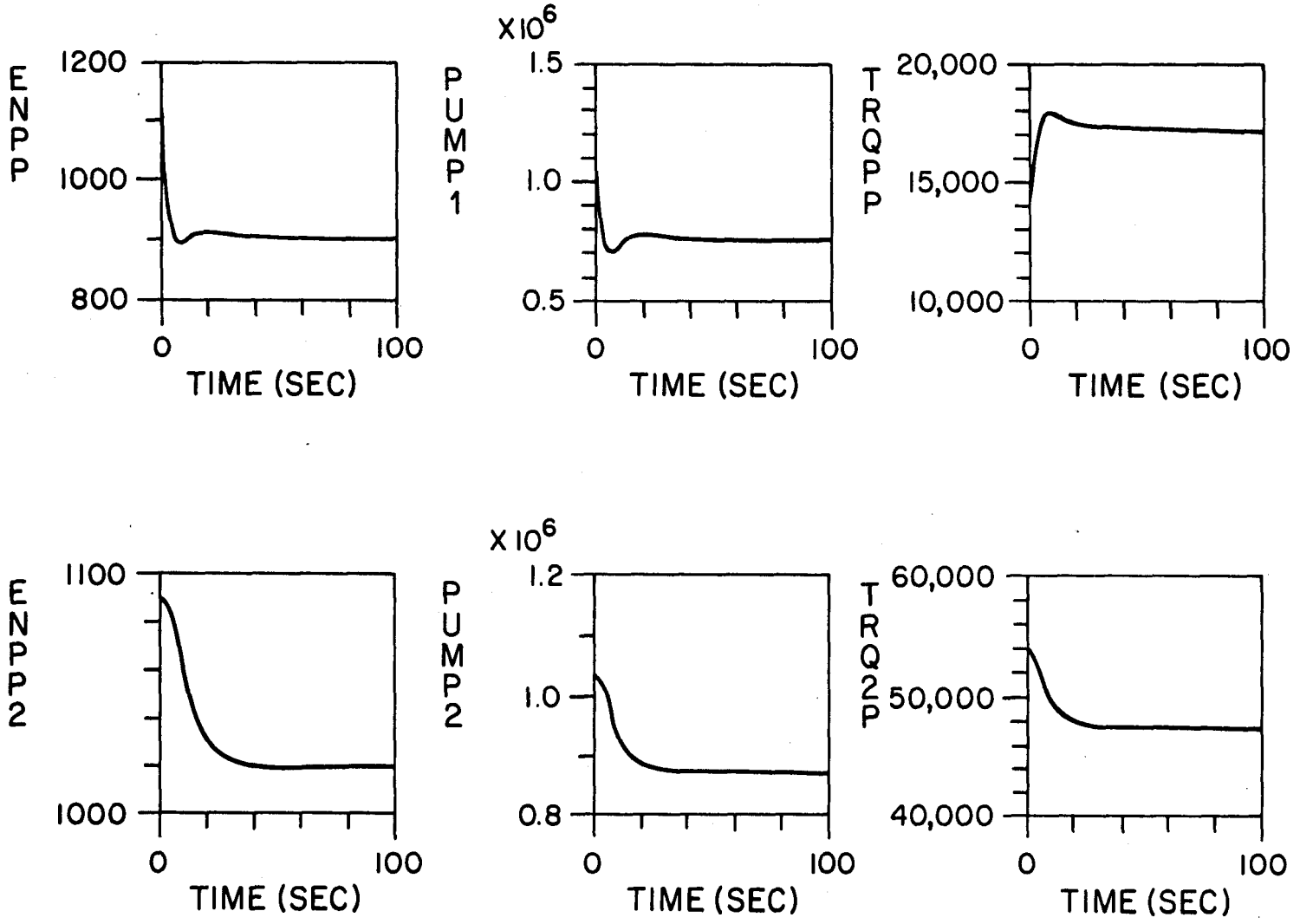

Fig. 3.7 10 Percent Deviation of Speed in Loop One - FFTF

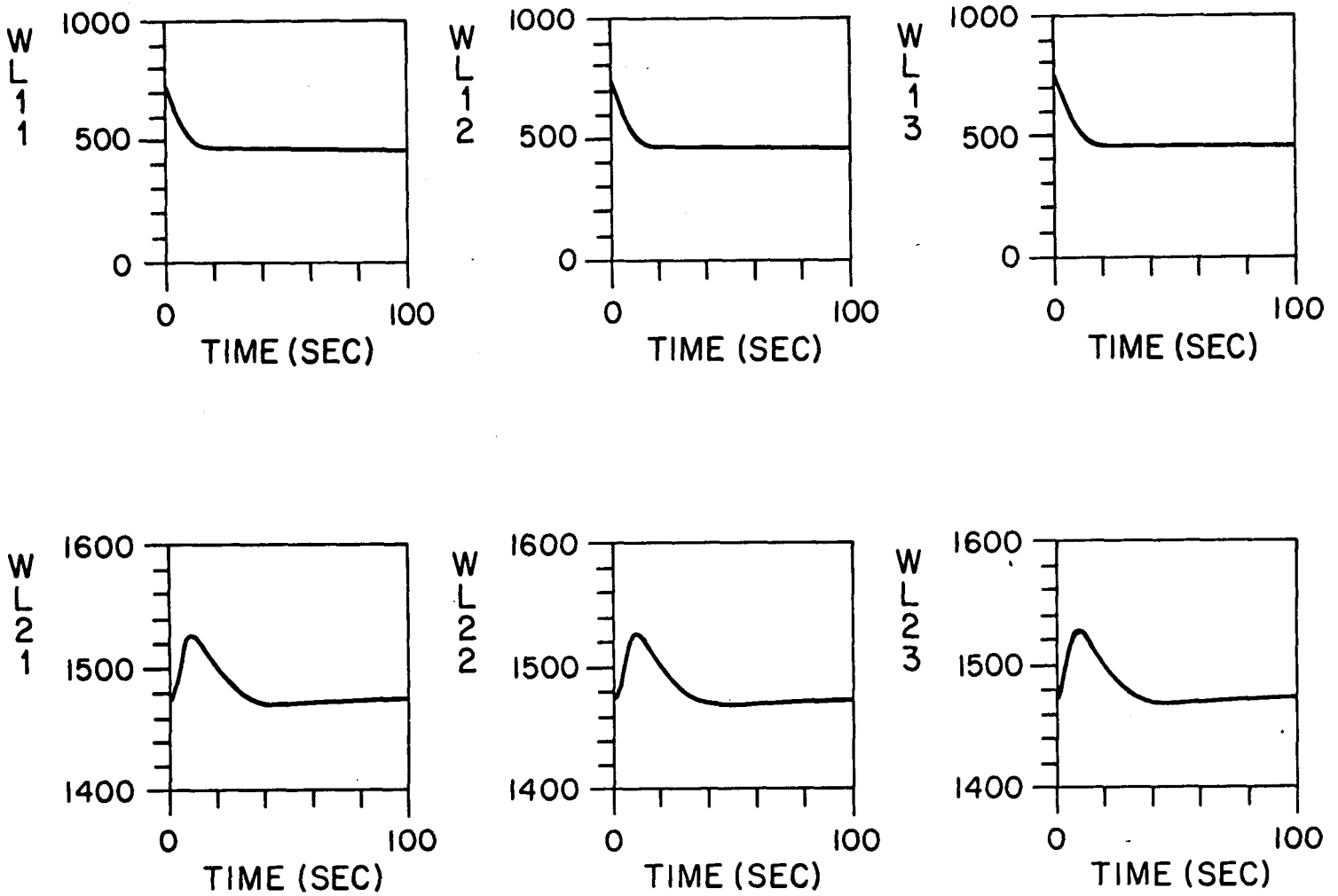

Fig. 3.7 -- Continued 10 Percent Deviation of Speed in Loop One - FFTF

CHAPTER 4

CONCLUSION

A single-phase centrifugal pump model for analysis of system transients in LMFBR plants has been presented, where homologous characteristic curves are used to predict the behavior of the pump during operating transients. The pump model has been coupled to BRENDA and FFTF to conduct the following transients:

For BRENDA

1. Primary pump coastdown to natural circulation coupled with scram failure.
2. 10 percent deviation of primary speed with plant controllers incorporated.

For FFTF

1. 10 percent deviation of primary speed.

From calculated results for the tests conducted, the following inferences are derived:

1. Representation of pump characteristics for all regions of operation forms an essential part of the pump model.
2. Frictional losses in the pump become very important under decreased speed and flow conditions. This is clearly shown in Figure 3.6 where a decrease in ENPP causes the torque TRQPP to increase.

APPENDIX A

Pump Performance Curves Coefficients

Head

The polynomial equations are of the form

$$\frac{h}{\alpha^2} = c_o + c_1 \frac{\nu}{\alpha} + c_2 \left(\frac{\nu}{\alpha}\right)^2 + c_3 \left(\frac{\nu}{\alpha}\right)^3 + c_4 \left(\frac{\nu}{\alpha}\right)^2 + c_5 \left(\frac{\nu}{\alpha}\right)^5$$

for HAN, HAD, HAT, HAR (A-1)

and

$$\frac{h}{\nu^2} = c_o + c_1 \frac{\alpha}{\nu} + c_2 \left(\frac{\alpha}{\nu}\right)^2 + c_3 \left(\frac{\alpha}{\nu}\right)^3 + c_4 \left(\frac{\alpha}{\nu}\right)^4 + c_5 \left(\frac{\alpha}{\nu}\right)^5$$

for HVN, HVD, HVT, HVR (A-2)

The values of the coefficients for all regions are listed in Table A.I.

Torque

The polynomial equations are of the form

$$\frac{\beta}{\alpha^2} = c_o + c_1 \frac{\nu}{\alpha} + c_2 \left(\frac{\nu}{\alpha}\right)^2 + c_3 \left(\frac{\nu}{\alpha}\right)^3 + c_4 \left(\frac{\nu}{\alpha}\right)^4 + c_5 \left(\frac{\nu}{\alpha}\right)^5$$

for BAN, BAD, BAT, BAR (A-3)

and

$$\frac{\beta}{\nu^2} = c_o + c_1 \frac{\alpha}{\nu} + c_2 \left(\frac{\alpha}{\nu}\right)^2 + c_3 \left(\frac{\alpha}{\nu}\right)^3 + c_4 \left(\frac{\alpha}{\nu}\right)^4 + c_5 \left(\frac{\alpha}{\nu}\right)^5$$

for BVN, BVD, BVT, BVR (A-4)

The values of the coefficients for all regions are listed in Table A.II.

Table A.I Head Polynomial Coefficients

Curves / Coefficients	HVN	HAN + HAD	HVD	HVT	HAT	HAR	HVR
C_o	-0.55392	1.264041	0.68211	0.68211	0.62307	0.62307	-0.55392
C_1	0.85376	0.061907	0.43961	-0.46132	0.20178	0.14665	0.66362
C_2	0.82906	-0.17327	0.68459	0.92592	-0.30242	-4.1896	-0.036081
C_3	-3.7106	-0.57294	-0.24701	-0.4308	0.76603	-2.4828	-0.93928
C_4	7.0593	0.033762	0.63156	0.50845	-0.48077	0.89730	-0.57381
C_5	-3.4776	0.3865	-0.20833	-0.22436	0.19231	0.0	0.0

Table A.II Torque Polynomial Coefficients

Curves / Coefficients	BVN	BAN + BAD	BVD	BVT	BAT	BAR	BVR
C_o	-0.3711	0.447841	0.8658	0.8658	-0.68468	-0.684	-0.3711
C_1	0.41741	0.5065	0.28437	-0.60816	1.8495	2.0342	2.3716
C_2	3.8511	0.59643	-0.22348	3.1497	0.96871	-0.95477	-0.56147
C_3	-7.6752	-0.64055	0.45083	-4.3647	-8.9653	-0.42286	0.0
C_4	7.0695	-0.025531	-0.70586	10.418	12.045	0.0	0.0
C_5	-2.2917	0.11531	0.21562	-4.0064	-4.7546	0.0	0.0

REFERENCES

Addition, S. L., et al., "Simulation of the overall FFTF Plant performance," HEDL TC-556, Westinghouse Hanford Company 1976.

Batenburg, A., Westinghouse Advanced Reactors Division, private communication, March 1978.

Donsky, B., "Complete Pump Characteristics and the Effects of Specific Speed on Hydraulic Transients," ASME Transactions, Journal of Basic Engineering, December 1967, p. 685-696.

Hetrick, D. L., and G. W. Sowers, "BRENDA, a Dynamic Simulation for a Sodium-Cooled Fast Reactor Power Plant," NUREG/CR-0244, University of Arizona EES-010-3, 1978. *

Knapp, R. T., "Complete Characteristics of Centrifugal Pumps and their use in Prediction of Transient Behavior," ASME Transactions, vol. 59, 1937, p. 683-689.

Madni, I. K., and E. Cazzoli, "A Single-Phase Pump Model for Analysis of LMFBR Heat Transport Systems," BNL-NUREG-50859 June 1978.

Mead, D. W., Hydraulic Machinery, McGraw-Hill Book Company, Inc., New York, N.Y. 1933, p. 313-318.

Parmakian, J., "Waterhammer Analysis," Prentice Hall, Inc. New York, N.Y., 1955.

RETRAN: "A Program for One-Dimensional Transient Thermal-Hydraulic Analysis of Complex Fluid Flow Systems," vol. 1, EPRI NP-408, January 1977.

Runstadler, P. W., "Review and Analysis of State-of-the-Art of Multiphase Pump Technology", Electric Power Research Institute, EPRI-159 February 1976.

Rust, J. H., Nuclear Power Plant Engineering, Haralson Publishing Company Buchanan, Georgia, 1979.

Sands, M., Graduate Student, Department of Nuclear Engineering, University of Arizona, private communication 1980.

Shinaishin, M. A., "Dynamic Simulation of a Sodium-Cooled Fast Reactor Power Plant", Ph.D. Dissertation, University of Arizona, Report No. NUREG-0110, 1976. *

Stepanoff, A. J., "Centrifugal and Axial Flow Pumps: Theory, Design and Application", 2nd Edition, John Wiley and Sons, Inc. New York, 1957.

Streeter, V. L., and E. B. Wylie, Hydraulic Transient, McGraw-Hill, New York, 1967.

*Available for purchase from the NRC/GPO Sales Program, U.S. Nuclear Regulatory Commission, Washington, DC 20555 and/or the National Technical Information Service, Springfield, VA 22161.

NRC FORM 335 (7-77) U.S. NUCLEAR REGULATORY COMMISSION

BIBLIOGRAPHIC DATA SHEET

1. REPORT NUMBER *(Assigned by DDC)*: NUREG/CR-2188

4. TITLE AND SUBTITLE *(Add Volume No., if appropriate)*: Simulation of Sodium Pumps for Nuclear Power Plants

2. *(Leave blank)*

3. RECIPIENT'S ACCESSION NO.

7. AUTHOR(S): H. O. Boadu

5. DATE REPORT COMPLETED: MONTH May YEAR 1981

9. PERFORMING ORGANIZATION NAME AND MAILING ADDRESS *(Include Zip Code)*:
Department of Nuclear and Energy Engineering
The University of Arizona
Tucson, Arizona 85721

DATE REPORT ISSUED: MONTH August YEAR 1981

6. *(Leave blank)*

8. *(Leave blank)*

12. SPONSORING ORGANIZATION NAME AND MAILING ADDRESS *(Include Zip Code)*:
Division of Accident Evaluation
Office of Nuclear Regulatory Research
U.S. Nuclear Regulatory Commission
Washington, DC 20555

10. PROJECT/TASK/WORK UNIT NO.

11. CONTRACT NO.: NRC FIN A4065

13. TYPE OF REPORT: Technical

PERIOD COVERED *(Inclusive dates)*: October 1, 1980 - May 1, 1981

15. SUPPLEMENTARY NOTES

14. *(Leave blank)*

16. ABSTRACT *(200 words or less)*

A single-phase pump model for analysis of transients in sodium cooled fast breeder nuclear power plants has been presented, where homologous characteristic curves are used to predict the behavior of the pump during operating transients. The pump model has been incorporated into BRENDA and FFTF; two system cases to simulate Clinch River Breeder Reactor Plant (CRBRP) and the Fast Flux Test Facility (FFTF) respectively. Two simulation test results for BRENDA which is one loop representation of a three loop plant have been presented. They are:

i) Primary pump coastdown to natural circulation coupled with scram failure.

ii) 10 percent deviation of primary speed with plant controllers incorporated.

In the case of FFTF, which is a two loop representation of three loop physical plant, the results of a 10 percent step decrease in one of the pumps will be presented.

17. KEY WORDS AND DOCUMENT ANALYSIS

17a. DESCRIPTORS

Nuclear reactors
digital simulation
systems codes
plant modeling

17b. IDENTIFIERS/OPEN-ENDED TERMS

18. AVAILABILITY STATEMENT: Unlimited

19. SECURITY CLASS *(This report)*: Unlimited

21. NO. OF PAGES

20. SECURITY CLASS *(This page)*: Unlimited

22. PRICE: S